Comput. Methods Appl. Mech. Engrg. 268 (2014) 160–177

Contents lists available at ScienceDirect

Comput. Methods Appl. Mech. Engrg.

journal homepage: www.elsevier.com/locate/cma

A posteriori error estimators for convection–diffusion eigenvalue problems ☆

J. Gedicke [a,*], C. Carstensen [b,c]

[a] Department of Mathematics and Center for Computation & Technology, Louisiana State University, Baton Rouge, LA 70803, USA
[b] Humboldt-Universität zu Berlin, Unter den Linden 6, 10099 Berlin, Germany
[c] Department of Computational Science and Engineering, Yonsei University, 120-749 Seoul, Republic of Korea

ARTICLE INFO

Article history:
Received 2 February 2011
Received in revised form 24 September 2012
Accepted 28 September 2012
Available online 14 September 2013

Dedicated to Professor Leszek F. Demkowicz on the occasion of his 60th birthday.

Keywords:
Convection–diffusion
Eigenvalue
Adaptive
Finite element method
Dual-weighted

ABSTRACT

A posteriori error estimators for convection–diffusion eigenvalue model problems are discussed in Heuveline and Rannacher (2001) [17] in the context of the dual-weighted residual method (DWR). This paper directly addresses the variational formulation rather than the non-linear ansatz of Becker and Rannacher for some convection–diffusion model problem and presents a posteriori error estimators for the eigenvalue error based on averaging techniques. Two different postprocessing techniques attached to the DWR paradigm plus two new dual-weighted a posteriori error estimators are also presented. The first new estimator utilises an auxiliary Raviart–Thomas mixed finite element method and the second exploits an averaging technique in combination with ideas of DWR. The six a posteriori error estimators are compared in three numerical examples and illustrate reliability and efficiency and the dependence of generic constants on the size of the eigenvalue or the convection coefficient.

1. Introduction

While the numerical approximation of eigenvalues of symmetric second-order elliptic partial differential equations (PDEs) with real eigenpairs is relatively well understood, much less is known about non-symmetric problems with possibly complex eigenvalues. A posteriori error estimators for symmetric eigenvalue problems can be found in [13,20,22,23,31]. The convergence of the adaptive finite element method (AFEM) for the symmetric case is considered in [9,14,15,28]. A posteriori error estimators for some non-symmetric eigenvalue problems can be found in [11,17,18]. It is the aim of this paper to review the results of Heuveline and Rannacher in a direct approach rather than in the non-linear setting of the DWR paradigm following [1,2,17]. These results are also applicable to the averaging techniques as for the symmetric eigenvalue problem in [22]. Numerical experiments indicate that the efficiency indices for the residual-type a posteriori error estimators depend strongly on the convection coefficient β. Therefore, this paper investigates the dual-weighted residual paradigm from Becker and Rannacher [2,3,1] and presents two new dual-weighted a posteriori error estimators. The first new estimator is based on the Raviart–Thomas mixed finite element method (MFEM) [6,27] of first-order and the second one on averaging techniques. Hence, they are named dual-weighted mixed (DWM) and dual-weighted averaging (DWA) a posteriori estimators. The paper

☆ Supported by the German Research Foundation (DFG) Research Center MATHEON "Mathematics for key technologies", the World Class University (WCU) program through the National Research Foundation of Korea (NRF) funded by the Ministry of Education, Science and Technology R31-2008-000-10049-0, and the graduate school BMS "Berlin Mathematical School".

* Corresponding author. Tel.: +1 225 578 7073.
E-mail addresses: jgedicke@math.lsu.edu (J. Gedicke), cc@math.hu-berlin.de (C. Carstensen).

0045-7825/$ - see front matter © 2013 Elsevier B.V. All rights reserved.
http://dx.doi.org/10.1016/j.cma.2012.09.018

presents numerical evidence that the DWR methodology in combination with the L^2 interpolation scheme of [32] is empirical reliable and efficient for unstructured triangular meshes while [17] is restricted to structured meshes because of the approximation of the weights by second-order difference quotients.

The convection–diffusion model eigenvalue problem reads: Seek an eigenpair $(\lambda, u) \in \mathbb{C} \times \{H_0^1(\Omega;\mathbb{C}) \cap H_{loc}^2(\Omega;\mathbb{C})\}$ with

$$-\Delta u + \beta \cdot \nabla u = \lambda u \quad \text{in } \Omega. \tag{1.1}$$

The given data $\beta \in H(div,\Omega;\mathbb{R}^2)$ is assumed to be divergence free in the bounded Lipschitz domain $\Omega \subseteq \mathbb{R}^2$, i.e., $\int_\Omega v\, div\, \beta\, dx = 0$ for all $v \in V := H_0^1(\Omega;\mathbb{C})$.

The weak problem considers the two complex Hilbert spaces V with energy norm $|||\cdot||| = |\cdot|_{H^1(\Omega;\mathbb{C})}$ (which is a norm on V) and $W := L^2(\Omega;\mathbb{C})$ with norm $\|\cdot\|_{L^2(\Omega;\mathbb{C})}$. The weak form reads: Seek an eigenpair $(\lambda, u) \in \mathbb{C} \times V$ with $\|u\| = 1$ such that

$$a(u, v) = \lambda b(u, v) \quad \text{for all } v \in V. \tag{1.2}$$

The bilinear form $a(\cdot,\cdot)$ is elliptic and continuous in V and the bilinear form $b(\cdot,\cdot)$ is continuous, symmetric and positive definite, and hence induces a norm $\|\cdot\| := b(\cdot,\cdot)^{1/2}$ on W. For the above model problem, $\|\cdot\| = \|\cdot\|_{L^2(\Omega;\mathbb{C})}$ and the bilinear forms (where $\overline{(\cdot)}$ denotes complex conjugation) read

$$a(u, v) = \int_\Omega (\nabla u \cdot \nabla \overline{v} + (\beta \cdot \nabla u)\overline{v})\, dx \qquad \text{and} \qquad b(u, v) = \int_\Omega u \overline{v}\, dx.$$

Since β is assumed to be divergence free, an integration by parts yields

$$\int_\Omega (\beta \cdot \nabla v)\overline{v}\, dx = -\int_\Omega (\beta \cdot \nabla \overline{v}) v\, dx.$$

Hence, for all $v \in V$, it holds that

$$|||v|||^2 = \operatorname{Re} a(v, v).$$

Thus, the ellipticity constant (which is one) of the bilinear form $a(\cdot,\cdot)$ is independent of β.

The analysis of the non-symmetric eigenvalue problem requires the dual eigenvalue problem: Seek a (dual) eigenpair $(\lambda^*, u^*) \in \mathbb{C} \times V$ with $\|u^*\| = 1$ such that

$$a(v, u^*) = \overline{\lambda^*} b(v, u^*) \quad \text{for all } v \in V.$$

Since the embedding of V in W is continuous and compact, the spectral theory for compact operators [19,24] is applicable. The Riesz-Schauder theorem shows that the primal and dual spectra consist of finite or countable infinite many eigenvalues with no finite accumulation point. In particular, the algebraic multiplicities are finite.

Throughout this paper, suppose that λ is a simple eigenvalue in the sense that the algebraic multiplicity and hence the geometric multiplicity is one and that λ is well separated from the remaining part of the spectrum.

Given any finite-dimensional subspace $V_\ell \subset V$, the discrete problems read: Seek primal and dual (discrete) eigenpairs (λ_ℓ, u_ℓ) and $(\lambda_\ell^*, u_\ell^*)$ with $\|u_\ell\| = 1 = \|u_\ell^*\|$ such that

$$a(u_\ell, v_\ell) = \lambda_\ell b(u_\ell, v_\ell) \quad \text{for all } v_\ell \in V_\ell \qquad \text{and} \qquad a(v_\ell, u_\ell^*) = \overline{\lambda_\ell^*} b(v_\ell, u_\ell^*) \quad \text{for all } v_\ell \in V_\ell. \tag{1.3}$$

The primal and dual eigenvalues λ_j and λ_j^* as well as the primal and dual discrete eigenvalues $\lambda_{\ell,j}$ and $\lambda_{\ell,j}^*$ are connected by

$$\lambda_j = \overline{\lambda_j^*} \quad \text{for } j = 1, 2, 3, \ldots \qquad \text{and} \qquad \lambda_{\ell,j} = \overline{\lambda_{\ell,j}^*} \quad \text{for all } j = 1, \ldots, \dim(V_\ell).$$

The abstract a priori theory yields the following upper bounds in terms of the maximal mesh-size H_ℓ,

$$|\lambda - \lambda_\ell| \lesssim H_\ell^{s_1+s_2}, \quad |||u - u_\ell||| \lesssim H_\ell^{s_1}, \quad |||u^* - u_\ell^*||| \lesssim H_\ell^{s_2},$$

where $0 < s_1 \leqslant 1$ and $0 < s_2 \leqslant 1$ depend on the regularity of the primal and dual eigenfunctions [[24], Chapter 10.3]. This paper employs standard notation on Lebesgue and Sobolev spaces and norms. Moreover, $x \lesssim y$ denotes an estimate $x \leqslant Cy$ with some generic constant $C > 0$, which is independent of the maximal mesh-size H_ℓ. Similarly $x \approx y$ abbreviates the inequalities $x \lesssim y$ and $y \lesssim x$.

The outline of the remaining parts of this paper is a follows. In Section 2 an optimal error estimate for the eigenvalue error is derived. For this, the basic algebraic properties and identities of the non-symmetric eigenvalue problem are reviewed. In contrast to [17], the direct variational formulation is used, rather then the more general non-linear DWR framework of Becker and Rannacher [1,2]. The weak regularity assumptions and the suboptimal L^2 error estimate of [17] prove the L^2 contribution to the residual identity to be of higher-order. Section 3 summarises some old and some new results on several a posteriori error estimators, namely the residual, the averaging, and the dual-weighted DWR1, DWR2, DWM and DWA a posteriori error estimators. Section 4 describes the adaptive finite element method, the interpolation scheme, used for the calculation of the weights, and the computation of the error estimators. In Section 5 the error estimators are compared in numerical benchmarks on three different domains for higher eigenvalues and various convection coefficients. Section 6 draws some conclusions.

2. Algebraic properties

This section is devoted with the primal and dual residual and the estimation of the eigenvalue and energy error in the primal and dual eigenfunctions.

For the primal and dual discrete eigenpairs (λ_ℓ, u_ℓ) and $(\lambda_\ell^*, u_\ell^*)$, the residuals are defined

$$\mathrm{Res}_\ell := a(u_\ell, \cdot) - \lambda_\ell b(u_\ell, \cdot) \in V^* \qquad \text{and} \qquad \mathrm{Res}_\ell^* := a(\cdot, u_\ell^*) - \overline{\lambda}_\ell^* b(\cdot, u_\ell^*) \in V^*$$

for the dual space V^* of V. Notice that $V_\ell \subset \ker(\mathrm{Res}_\ell)$ and $V_\ell \subset \ker(\mathrm{Res}_\ell^*)$.

It is the goal of this section to derive the following optimal error estimate for the eigenvalue error of simple eigenvalues

$$|\lambda - \lambda_\ell| \lesssim |||\mathrm{Res}_\ell|||_*^2 + |||\mathrm{Res}_\ell^*|||_*^2 \tag{2.1}$$

which is valid only for $H_\ell \ll 1$. Throughout this paper let $e_\ell := u - u_\ell$ and $e_\ell^* := u^* - u_\ell^*$.

Lemma 2.1 (*Primal–dual error residual identity*). *Suppose that (λ_ℓ, u_ℓ) and $(\lambda_\ell^*, u_\ell^*)$ are the discrete primal and discrete dual eigenpairs to the primal and dual eigenpairs (λ, u) and (λ^*, u^*). Then it holds that*

$$(\lambda - \lambda_\ell)\big(b(u, u^*) + b(u_\ell, u_\ell^*) - b(e_\ell, e_\ell^*)\big) = \mathrm{Res}_\ell(e_\ell^*) + \mathrm{Res}_\ell^*(e_\ell).$$

Proof. Direct algebraic manipulations and the definition of the residuals and using that $\lambda = \overline{\lambda^*}, \lambda_\ell = \overline{\lambda_\ell^*}$ leads to

$$\begin{aligned} a(u_\ell, u^* - u_\ell^*) - \lambda_\ell b(u_\ell, u^* - u_\ell^*) + a(u - u_\ell, u_\ell^*) - \overline{\lambda_\ell^*} b(u - u_\ell, u_\ell^*) &= a(u_\ell, u^*) - \lambda_\ell b(u_\ell, u^*) + a(u, u_\ell^*) - \overline{\lambda_\ell^*} b(u, u_\ell^*) \\ &= (\overline{\lambda^*} - \lambda_\ell) b(u_\ell, u^*) + (\lambda - \overline{\lambda_\ell^*}) b(u, u_\ell^*) \\ &= (\lambda - \lambda_\ell)(b(u, u^*) + b(u_\ell, u_\ell^*) - b(e_\ell, e_\ell^*)). \qquad \square \end{aligned}$$

Lemma 2.2. *Suppose that the maximal mesh-size H_ℓ tends to zero as $\ell \to \infty$, then*

$$\lim_{\ell \to \infty} b(e_\ell, e_\ell^*) = 0 \quad \text{and} \quad \lim_{\ell \to \infty} b(u_\ell, u_\ell^*) = b(u, u^*).$$

Proof. The convergence of $|||e_\ell|||$ and $|||e_\ell^*|||$ implies the convergence of $\|e_\ell\|$ and $\|e_\ell^*\|$ to zero as $\ell \to \infty$ because of the compact embedding. Hence, the assertions follow from $|b(e_\ell, e_\ell^*)| \leqslant \|e_\ell\| \|e_\ell^*\|$ and

$$|b(u, u^*) - b(u_\ell, u_\ell^*)| = |b(u - u_\ell, u^*) + b(u_\ell, u^* - u_\ell^*)| \leqslant \|e_\ell\| + \|e_\ell^*\|. \qquad \square$$

Remark 2.1. Since all eigenvalues converge as $H_\ell \to 0, \lambda_\ell$ is, as λ, a simple eigenvalue for sufficiently small H_ℓ. For a vector $z \in \mathbb{R}^m$ let z^H denotes its complex conjugate transposed vector. The condition number $1/|y_\ell^H B_\ell x_\ell|$ of the discrete eigenvalue λ_ℓ is defined for right and left eigenvectors x_ℓ and y_ℓ of the algebraic eigenvalue problems

$$A_\ell x_\ell = \lambda_\ell B_\ell x_\ell \quad \text{and} \quad y_\ell^H A_\ell = \overline{\lambda_\ell^*} y_\ell^H B_\ell,$$

with non-symmetric convection–diffusion matrix A_ℓ and symmetric positive definite mass matrix B_ℓ [16, Section 7.2.2]. It is known that $y_\ell^H B_\ell x_\ell \neq 0$ for simple eigenvalues and that $|y_\ell^H B_\ell x_\ell| \gg 0$ if the simple eigenvalue is well separated from the remaining part of the spectrum. Hence, for well separated simple eigenvalues considered in this paper, it is reasonable to assume $b(u, u^*) \neq 0$. Furthermore, $1/|b(u, u^*)|$ is the condition number of the continuous eigenvalue λ and

$$|b(u, u^*) + b(u_\ell, u_\ell^*) - b(e_\ell, e_\ell^*)| \longrightarrow 2\,|b(u, u^*)|$$

as $H_\ell \to 0$.

Suppose that λ is simple such that $b(u, u^*) \neq 0$ and let $\ell \gg 1$ be such that the maximal mesh-size H_ℓ of the triangulation $\mathcal{T}_\ell$ is sufficiently small, i.e.,

$$\max\{\|e_\ell\|, \|e_\ell^*\|\} < \min\{1, |b(u, u^*)|/2\}. \tag{2.2}$$

Then $|b(u, u^*)| < |b(u, u^*) + b(u_\ell, u_\ell^*) - b(e_\ell, e_\ell^*)| < 3$, where the lower bound follows from

$$\begin{aligned} |b(u, u^*) + b(u_\ell, u_\ell^*) - b(e_\ell, e_\ell^*)| &= |2b(u, u^*) - b(u, u^* - u_\ell^*) - b(u - u_\ell, u^*)| \\ &\geqslant 2\,|b(u, u^*)| - |b(u, u^* - u_\ell^*) + b(u - u_\ell, u^*)| \\ &\geqslant 2\,|b(u, u^*)| - \|u\| \|e_\ell^*\| - \|u^*\| \|e_\ell\| \\ &= 2\,|b(u, u^*)| - \|e_\ell^*\| - \|e_\ell\| \end{aligned}$$

and (2.2). Thus for simple eigenvalues λ it holds that

$$| \lambda - \lambda_\ell | \approx | \operatorname{Res}_\ell(e_\ell^*) + \operatorname{Res}_\ell^*(e_\ell) | . \tag{2.3}$$

This implies the suboptimal eigenvalue error estimate

$$| \lambda - \lambda_\ell | \lesssim |||\operatorname{Res}_\ell|||_* + |||\operatorname{Res}_\ell^*|||_*. \tag{2.4}$$

Remark 2.2. The proof of the following Lemma 2.3 applies a suboptimal L^2 error estimate that is based on the *weak regularity assumption* of the eigenvalue λ with the eigenspace $E(\lambda)$. That is a condition on

$$a_\lambda(\cdot,\cdot) = a(\cdot,\cdot) - \lambda b(\cdot,\cdot),$$

on the quotient space $V/E(\lambda)$ in the sense that

$$|||w||| \leqslant C_\lambda \sup_{v \in V/E(\lambda)} \frac{| a_\lambda(v,w) |}{|||v|||} \quad \text{for all } w \in V/E(\lambda).$$

The constant C_λ depends on the distance of λ to all other distinct eigenvalues and does not depend on the mesh-size. This weak regularity assumption implies the suboptimal L^2 error estimates [17, (70)–(71)]

$$\|e_\ell\| \lesssim |||\operatorname{Res}_\ell|||_* + | \lambda - \lambda_\ell | \qquad \text{and} \qquad \|e_\ell^*\| \lesssim |||\operatorname{Res}_\ell^*|||_* + | \lambda - \lambda_\ell | . \tag{2.5}$$

Lemma 2.3 (*Energy estimate*). *Suppose that $b(u,u^*) \neq 0$, the maximal mesh-size H_ℓ is sufficiently small according to (2.2), and (λ_ℓ, u_ℓ) and $(\lambda_\ell^*, u_\ell^*)$ are the discrete primal and discrete dual eigenpairs to the primal and dual eigenpairs (λ, u) and (λ^*, u^*). Then it holds that*

$$|||e_\ell||| + |||e_\ell^*||| \lesssim |||\operatorname{Res}_\ell|||_* + |||\operatorname{Res}_\ell^*|||_*.$$

Proof. Since $b(u,u) = 1 = b(u_\ell, u_\ell)$, the eigenvalue Eqs. (1.2) and (1.3) imply that

$$a(e_\ell, e_\ell) = \lambda + \lambda_\ell - \lambda b(u, u_\ell) - a(u_\ell, u).$$

The relation

$$\lambda_\ell b(u_\ell, u) = \lambda_\ell \overline{b(u, u_\ell)} = \lambda_\ell \operatorname{Re} b(u, u_\ell) - i\lambda_\ell \operatorname{Im} b(u, u_\ell)$$

leads to

$$a(e_\ell, e_\ell) = (\lambda + \lambda_\ell)(1 - \operatorname{Re} b(u, u_\ell)) + i(\lambda_\ell - \lambda)\operatorname{Im} b(u, u_\ell) + \lambda_\ell b(u_\ell, u) - a(u_\ell, u).$$

From $0 = \operatorname{Im}\|u_\ell\|^2 = \operatorname{Im} b(u_\ell, u_\ell)$ it follows that

$$a(e_\ell, e_\ell) = (\lambda + \lambda_\ell)(1 - \operatorname{Re} b(u, u_\ell)) + i(\lambda_\ell - \lambda)\operatorname{Im} b(u - u_\ell, u_\ell) + \lambda_\ell b(u_\ell, u) - a(u_\ell, u).$$

Since

$$2\operatorname{Re} b(u, u_\ell) = \|u\|^2 + \|u_\ell\|^2 - \|e_\ell\|^2 = 2 - \|e_\ell\|^2,$$

this implies

$$|||e_\ell|||^2 = \operatorname{Re} a(e_\ell, e_\ell) \leqslant |\operatorname{Res}_\ell(e_\ell)| + |\lambda - \lambda_\ell| \|e_\ell\| + \frac{| \lambda + \lambda_\ell |}{2} \|e_\ell\|^2. \tag{2.6}$$

The suboptimal estimates (2.4) and (2.5) imply

$$| \lambda - \lambda_\ell | + \|e_\ell\| \lesssim |||\operatorname{Res}_\ell|||_* + |||\operatorname{Res}_\ell^*|||_*. \tag{2.7}$$

Since $\|.\| \lesssim |||.|||$, the inequalities (2.6), (2.7) yield

$$|||e_\ell||| \lesssim |||\operatorname{Res}_\ell|||_* + |||\operatorname{Res}_\ell^*|||_*.$$

Similarly it follows that

$$|||e_\ell^*||| \lesssim |||\operatorname{Res}_\ell|||_* + |||\operatorname{Res}_\ell^*|||_*. \qquad \square$$

Theorem 2.4 (*Eigenvalue Error Estimate*). *Suppose that $b(u,u^*) \neq 0$, the maximal mesh-size H_ℓ is sufficiently small such that (2.2) holds and let (λ_ℓ, u_ℓ) and $(\lambda_\ell^*, u_\ell^*)$ be the discrete primal and discrete dual eigenpairs to the primal and dual eigenpairs (λ, u) and (λ^*, u^*) for the simple eigenvalue λ. Then it holds that*

$$|\lambda - \lambda_\ell| \lesssim |||\operatorname{Res}_\ell|||_*^2 + |||\operatorname{Res}_\ell^*|||_*^2.$$

Proof. The aforementioned estimate (2.3), the Cauchy–Schwarz inequality and Lemma 2.3 lead to

$$|\lambda - \lambda_\ell| \lesssim |\mathrm{Res}_\ell(e_\ell^*)| + |\mathrm{Res}_\ell^*(e_\ell)| \lesssim |||\mathrm{Res}_\ell|||_*^2 + |||\mathrm{Res}_\ell^*|||_*^2. \qquad \square$$

3. A posteriori error estimates

This section is devoted to the residual, averaging and dual-weighted residual a posteriori error estimators for the eigenvalue error of simple eigenvalues. The first two residual and averaging based a posteriori error estimators make use of Theorem 2.4

$$|\ \lambda - \lambda_\ell\ | \ \lesssim |||\mathrm{Res}_\ell|||_*^2 + |||\mathrm{Res}_\ell^*|||_*^2.$$

Here, the dual norms of the primal and dual residuals are bounded separately. The DWR based a posteriori error estimators are derived from the asymptotic estimate (2.3) for simple eigenvalues,

$$|\ \lambda - \lambda_\ell\ | \approx |\ \mathrm{Res}_\ell(e_\ell^*) + \mathrm{Res}_\ell^*(e_\ell)\ |,$$

where the constant tends to $1/(2\ |\ b(u,u^*)\ |)$ as $H_\ell \to 0$. In general the dual-weighted error estimators avoid any additional inequality, such as approximation properties, with unknown constants. Thus, they are robust with respect to strong convection which is also confirmed by the numerical examples in Section 5. One question that arises from the computation of $\mathrm{Res}_\ell(e_\ell^*)$ or $\mathrm{Res}_\ell^*(e_\ell)$ is the calculation of the unknown errors e_ℓ and e_ℓ^*. The rather heuristic approach of [1] states that it is numerically reliable and efficient to approximate these quantities which occur only in the weights. The idea is that one does not need to approximate the weights with higher accuracy than the size of the residual terms. In practice, the unknown primal and dual solutions u, u^* are replaced by solutions of a higher-order method or by higher-order interpolation. In Section 4 a higher-order interpolation ansatz for general triangular meshes is described which leads to numerically reliable and efficient dual-weighted a posteriori error estimators.

Throughout this paper, suppose $(\mathcal{T}_\ell)_\ell$ is a family of shape-regular triangulations of Ω into triangles, i.e. each $T \in \mathcal{T}_\ell$ is a closed triangle, $\overline{\Omega} = \bigcup_{T\in\mathcal{T}_\ell} T$, for any two distinct triangles $T_1, T_2 \in \mathcal{T}_\ell$ and $T_1 \cap \mathcal{T}_2$ is either empty, a common vertex or a common side. Suppose that the minimal angle of every triangle is uniformly bounded from below. The conforming finite element space of order $k \in \mathbb{N}$ for the triangulation $\mathcal{T}_\ell$ is defined by

$$\mathcal{P}_k(\mathcal{T}_\ell) := \left\{ v \in H^1(\Omega;\mathbb{C}) : \forall T \in \mathcal{T}_\ell,\ v_T \text{ is polynomial of degree } \leqslant k \right\}.$$

Let $V_\ell := \mathcal{P}_1(\mathcal{T}_\ell) \cap V$ and $h_\ell \in \mathcal{P}_0(\mathcal{T}_\ell)$ be such that $h_{\ell|T} := \mathrm{diam}(T)$ for all $T \in \mathcal{T}_\ell$. Given a triangulation $\mathcal{T}_\ell$, define $\mathcal{E}_\ell$ as the set of inner edges and $\mathcal{N}_\ell$ as the set of inner nodes. Let $h_T := \mathrm{diam}(T)$ for $T \in \mathcal{T}_\ell$ and $h_E := \mathrm{diam}(E)$ for $E \in \mathcal{E}_\ell$. The jump of the discrete gradient $\nabla u_\ell \in \mathcal{P}_0(\mathcal{T}_\ell)^2$ in normal direction ν_E along an inner edge $\partial T_+ \cap \partial T_- = E \in \mathcal{E}_\ell$, for $T_+, T_- \in \mathcal{T}_\ell$, is denoted by $[\![\nabla u_\ell]\!] \cdot \nu_E = \nabla u_\ell|_{T_+} \cdot \nu_E - \nabla u_\ell|_{T_-} \cdot \nu_E$ and $[\![\nabla u_\ell]\!] \cdot \nu_E = 0$ for boundary edges $E \subset \partial\Omega$.

3.1. Residual estimator

The first a posteriori error estimator is the residual error estimator from [17].

Lemma 3.1. *Let (λ_ℓ, u_ℓ) and $(\lambda_\ell^*, u_\ell^*)$ be the discrete primal and discrete dual eigenpairs to the primal and dual eigenpairs (λ, u) and (λ^*, u^*). Then it holds that*

$$|||\mathrm{Res}_\ell|||_*^2 \lesssim \sum_{T\in\mathcal{T}_\ell} h_T^2 \|\beta\cdot\nabla u_\ell - \lambda_\ell u_\ell\|_{L^2(T)}^2 + \sum_{E\in\mathcal{E}_\ell} h_E \|[\![\nabla u_\ell]\!]\cdot\nu_E\|_{L^2(E)}^2,$$
$$|||\mathrm{Res}_\ell^*|||_*^2 \lesssim \sum_{T\in\mathcal{T}_\ell} h_T^2 \|-\beta\cdot\nabla \overline{u_\ell^*} - \overline{\lambda_\ell^* u_\ell^*}\|_{L^2(T)}^2 + \sum_{E\in\mathcal{E}_\ell} h_E \|[\![\nabla \overline{u_\ell^*}]\!]\cdot\nu_E\|_{L^2(E)}^2.$$

Proof. Let v_ℓ denote the Scott-Zhang interpolation of v onto V_ℓ. Then it holds that

$$\begin{aligned}
\mathrm{Res}_\ell(v) &= \mathrm{Res}_\ell(v - v_\ell) = a(u_\ell, v - v_\ell) - \lambda_\ell b(u_\ell, v - v_\ell)\\
&= \sum_{T\in\mathcal{T}_\ell} \int_T \nabla u_\ell \cdot \nabla(\overline{v - v_\ell}) + (\beta\cdot\nabla u_\ell)(\overline{v - v_\ell})dx - \lambda_\ell \int_T u_\ell(\overline{v - v_\ell})dx\\
&= \sum_{T\in\mathcal{T}_\ell} \int_T (\beta\cdot\nabla u_\ell - \lambda_\ell u_\ell)(\overline{v - v_\ell})dx + \sum_{E\in\mathcal{E}_\ell} \int_E ([\![\nabla u_\ell]\!]\cdot\nu_E)(\overline{v - v_\ell})ds.
\end{aligned}$$

The approximation properties of the interpolation operator [29]

$$\sum_{T\in\mathcal{T}_\ell} \|h_T^{-1}(v - v_\ell)\|_{L^2(T)}^2 + \sum\nolimits_{E\in\mathcal{E}_\ell} \|h_E^{-1/2}(v - v_\ell)\|_{L^2(E)}^2 \lesssim |||v|||^2, \tag{3.1}$$

and the Cauchy–Schwarz inequality yield

$$\mathrm{Res}_\ell(v) \leqslant \sum_{T\in\mathcal{T}_\ell} h_T\|\beta\cdot\nabla u_\ell - \lambda_\ell u_\ell\|_{L^2(T)}\|h_T^{-1}(v-v_\ell)\|_{L^2(T)} + \sum_{E\in\mathcal{E}_\ell} h_E^{1/2}\|[\nabla u_\ell]\cdot\nu_E\|_{L^2(E)}\|h_E^{-1/2}(v - v_\ell)\|_{L^2(E)} \lesssim \left(\sum_{T\in\mathcal{T}_\ell} h_T^2\|\beta\cdot\nabla u_\ell - \lambda_\ell u_\ell\|_{L^2(T)}^2\right)^{1/2} |||v||| + \left(\sum_{E\in\mathcal{E}_\ell} h_E\|[\nabla u_\ell]\cdot\nu_E\|_{L^2(E)}^2\right)^{1/2} |||v|||.$$

For the second assertion notice that the dual bilinear form $a^*(u^*,\cdot) := a(\cdot,u^*)$ reads in the model problem

$$a^*(u^*,v) = a(v,u^*) = \int_\Omega (\nabla v\cdot\nabla\overline{u^*} + (\beta\cdot\nabla v)\overline{u^*})\,dx.$$

An integration by parts leads to

$$a^*(u^*,v) = \int_\Omega (\nabla\overline{u^*}\cdot\nabla v - (\beta\cdot\nabla\overline{u^*})v)\,dx \quad \text{for all } v\in V.$$

The same arguments as for the first assertion lead to the assertion for $|||\mathrm{Res}_\ell^*|||$. □

3.2. Averaging estimator

The averaging technique concerns operators

$$A : \mathcal{P}_0(\mathcal{T}_\ell)^2 \to \{V_\ell^2 \cap \mathcal{C}(\Omega)^2\},$$

with the model example

$$A(\nabla u_\ell) := \sum_{z\in\mathcal{N}_\ell} \frac{1}{|\omega_z|}\left(\int_{\omega_z}\nabla u_\ell\,dx\right)\varphi_z.$$

Here and throughout this paper, φ_z denotes the nodal basis function for an inner node $z\in\mathcal{N}_\ell$. Alternative averaging operators from [7] could be employed as well.

Lemma 3.2. *Let (λ_ℓ,u_ℓ) and $(\lambda_\ell^*,u_\ell^*)$ be the discrete primal and discrete dual eigenpairs to the primal and dual eigenpairs (λ,u) and (λ^*,u^*). Then it holds that*

$$|||\mathrm{Res}_\ell|||_* \lesssim \|h_\ell(-div(A(\nabla u_\ell)) + \beta\cdot\nabla u_\ell - \lambda_\ell u_\ell)\|_{L^2(\Omega)} + \|A(\nabla u_\ell) - \nabla u_\ell\|_{L^2(\Omega)},$$
$$|||\mathrm{Res}_\ell^*|||_* \lesssim \|h_\ell(-div(A(\nabla\overline{u_\ell^*})) - \beta\cdot\nabla\overline{u_\ell^*} - \overline{\lambda_\ell^* u_\ell^*})\|_{L^2(\Omega)} + \|A(\nabla\overline{u_\ell^*}) - \nabla\overline{u_\ell^*}\|_{L^2(\Omega)}.$$

Proof. As in the previous lemma, let v_ℓ denote the Scott–Zhang interpolation of v onto V_ℓ, since $A(\nabla u_\ell)$ is globally continuous the divergence theorem can be applied. This yields

$$\begin{aligned}\mathrm{Res}_\ell(v) &= \mathrm{Res}_\ell(v-v_\ell) = a(u_\ell, v-v_\ell) - \lambda_\ell b(u_\ell, v-v_\ell)\\ &= \int_\Omega(\nabla u_\ell - A(\nabla u_\ell))\cdot\nabla(\overline{v-v_\ell})dx - \int_\Omega div(A(\nabla u_\ell))(\overline{v-v_\ell})dx + \int_\Omega(\beta\cdot\nabla u_\ell - \lambda_\ell u_\ell)(\overline{v-v_\ell})dx.\end{aligned}$$

Hölder's inequality leads to

$$\mathrm{Res}_\ell(v) \leqslant \sum_{T\in\mathcal{T}_\ell}\left(h_T\|-div(A(\nabla u_\ell)) + \beta\cdot\nabla u_\ell - \lambda_\ell u_\ell\|_{L^2(T)}\|h_T^{-1}(v-v_\ell)\|_{L^2(T)}\right) + \sum_{T\in\mathcal{T}_\ell}\|\nabla u_\ell - A(\nabla u_\ell)\|_{L^2(T)}\|\nabla(v-v_\ell)\|_{L^2(T)}.$$

Using the stability and the approximation property (3.1)

$$\sum_{T\in\mathcal{T}_\ell}\|\nabla v_\ell\|_{L^2(T)}^2 \lesssim |||v|||^2 \quad\text{and}\quad \sum_{T\in\mathcal{T}_\ell}\|h_T^{-1}(v-v_\ell)\|_{L^2(T)}^2 \lesssim |||v|||^2,$$

together with the Cauchy–Schwarz inequality yield

$$\mathrm{Res}_\ell(v) \lesssim \left(\|h_\ell(-div(A(\nabla u_\ell)) + \beta\cdot\nabla u_\ell - \lambda_\ell u_\ell)\|_{L^2(\Omega)} + \|A(\nabla u_\ell) - \nabla u_\ell\|_{L^2(\Omega)}\right)|||v|||.$$

In the same way one proves the assertion for $|||\mathrm{Res}_\ell^*|||$. □

3.3. DWR1 estimator

The first DWR a posteriori error estimator (DWR1) is derived from the DWR ansatz as in [17] or [1] plus a result from [8].

Lemma 3.3. *Let the eigenfunctions $u, u^* \in H^2(\Omega) \cap H^3(\mathcal{T}_\ell)$, $H^3(\mathcal{T}_\ell)$ denote the broken space of piecewise H^3 Sobolev functions, (λ_ℓ, u_ℓ) and $(\lambda_\ell^*, u_\ell^*)$ be the discrete primal and discrete dual eigenpairs to the primal and dual eigenpairs (λ, u) and (λ^*, u^*), and*

$$\begin{aligned} \eta_T &:= \|\beta \cdot \nabla u_\ell - \lambda_\ell u_\ell\|_{L^2(T)} + h_T^{-1/2} \|[\nabla u_\ell] \cdot \nu_E\|_{L^2(\partial T)}, \\ \eta_T^* &:= \| - \beta \cdot \nabla \overline{u_\ell^*} - \overline{\lambda_\ell^* u_\ell^*}\|_{L^2(T)} + h_T^{-1/2} \|[\nabla \overline{u_\ell^*}] \cdot \nu_E\|_{L^2(\partial T)}. \end{aligned} \tag{3.2}$$

Then it holds that

$$|\operatorname{Res}_\ell(e_\ell^*)| + |\operatorname{Res}_\ell^*(e_\ell)| \lesssim \sum_{T \in \mathcal{T}_\ell} h_T^{3/2} \eta_T \|[\nabla u_\ell^*] \cdot \nu_E\|_{L^2(\bigcup \mathcal{E}_{\Omega_T})} + \sum_{T \in \mathcal{T}_\ell} h_T^{3/2} \eta_T^* \|[\nabla u_\ell] \cdot \nu_E\|_{L^2(\bigcup \mathcal{E}_{\Omega_T}))} + \mathrm{HOT}$$

for suitable fixed subsets $\Omega_T \subseteq \Omega$, which contain $T \in \mathcal{T}_\ell$, with skeleton $\bigcup \mathcal{E}_{\Omega_T}$, and a higher-order term

$$\mathrm{HOT} := \sum_{T \in \mathcal{T}_\ell} h_T^2 \eta_T \|\nabla e_\ell^*\|_{L^2(\Omega_T)} + \sum_{T \in \mathcal{T}_\ell} h_T^2 \eta_T^* \|\nabla e_\ell\|_{L^2(\Omega_T)}.$$

Proof. Suppose $u \in H^2(\Omega)$, then integration by parts and Hölder's inequality show that

$$\begin{aligned} \operatorname{Res}_\ell(v) &= \sum_{T \in \mathcal{T}_\ell} \int_T \nabla u_\ell \cdot \nabla(\overline{v - v_\ell}) + (\beta \cdot \nabla u_\ell - \lambda_\ell u_\ell)(\overline{v - v_\ell}) dx \\ &\leqslant \sum_{T \in \mathcal{T}_\ell} h_T^{-1/2} \|[\nabla u_\ell] \cdot \nu_E\|_{L^2(\partial T)} h_T^{1/2} \|v - v_\ell\|_{L^2(\partial T)} + \|\beta \cdot \nabla u_\ell - \lambda_\ell u_\ell\|_{L^2(T)} \|v - v_\ell\|_{L^2(T)} \leqslant \sum_{T \in \mathcal{T}_\ell} \eta_T \omega_T. \end{aligned}$$

Here, η_T is as defined in (3.2) and

$$\omega_T := \|v - v_\ell\|_{L^2(T)} + h_T^{1/2} \|v - v_\ell\|_{L^2(\partial T)}.$$

Let $v_\ell = \mathcal{I}_\ell v \in V_\ell$ be the nodal interpolant of v. The interpolation estimate [5]

$$\|v - \mathcal{I}_\ell v\|_{L^2(T)}^2 + h_T \|v - \mathcal{I}_\ell v\|_{L^2(\partial T)}^2 \lesssim h_T^4 \|D^2 v\|_{L^2(T)}^2$$

leads to

$$\operatorname{Res}_\ell(v) \lesssim \sum_{T \in \mathcal{T}_\ell} h_T^2 \eta_T \|D^2 v\|_{L^2(T)}.$$

In [17] $D^2 v$ is locally approximated on each quadrilateral Q by $D^2 v_\ell|_Q$ using finite differences. While this is an appropriate ansatz for structured meshes, for general triangular meshes considered here this is not suited. In [8] it is shown that $v \in H^3(\mathcal{T}_\ell)$ implies

$$\|D^2 v\|_{L^2(T)} \leqslant c_1 h_T^{-1/2} \|[\nabla v_\ell] \cdot \nu_E\|_{L^2(\bigcup \mathcal{E}_{\Omega_T}))} + c_2 \|\nabla(v - v_\ell)\|_{L^2(\Omega_T)}^{1/2}.$$

The constant c_1 depends on the shape of elements and c_2 on $\|v\|_{H^3(\Omega_T)}$. This leads to the estimate

$$|\operatorname{Res}_\ell(e_\ell^*)| \lesssim \sum_{T \in \mathcal{T}_\ell} h_T^{3/2} \eta_T \|[\nabla u_\ell^*] \cdot \nu_E\|_{L^2(\bigcup \mathcal{E}_{\Omega_T})} + \mathrm{HOT},$$

with higher-order term

$$\mathrm{HOT} = \sum_{T \in \mathcal{T}_\ell} h_T^2 \eta_T \|\nabla e_\ell^*\|_{L^2(\Omega_T)}.$$

Note that the jump term is formally equivalent to the energy norm and that HOT involves an extra factor of $h_T^{1/2}$ compared to the other term of the estimate. Following the argumentation for the primal residual yields the assertion for the dual residual

$$|\operatorname{Res}_\ell^*(e_\ell)| \lesssim \sum_{T \in \mathcal{T}_\ell} h_T^{3/2} \eta_T^* \|[\nabla u_\ell] \cdot \nu_E\|_{L^2(\bigcup \mathcal{E}_{\Omega_T})} + \mathrm{HOT},$$

with the higher-order term

$$\mathrm{HOT} = \sum_{T \in \mathcal{T}_\ell} h_T^2 \eta_T^* \|\nabla e_\ell\|_{L^2(\Omega_T)}. \qquad \square$$

Remark 3.1. From the theory in [8] it remains open to choose the fixed size of the patches Ω_T containing $T \in \mathcal{T}_\ell$. However, the numerical examples of Section 5 suggest, that, surprisingly, $\Omega_T = T$ and thus $\bigcup \mathcal{E}_{\Omega_T} = \partial T$ might be sufficient. This seems to be in agreement with [1].

3.4. DWR2 estimator

The second DWR estimator (DWR2) according to [1] reads as follows. Observe that this error estimator involves the unknown exact primal and dual errors e_ℓ and $\overline{e_\ell^*}$. In the numerical examples of Section 5, these errors will be approximated by the interpolation described in Section 4.

Lemma 3.4. *The unknown exact errors e_ℓ and $\overline{e_\ell^*}$ satisfy*

$$
\begin{aligned}
|\,\mathrm{Res}_\ell(e_\ell^*)+\mathrm{Res}_\ell^*(e_\ell)\,| = \Bigg| & \sum_{T\in\mathcal{T}_\ell}\int_T(\beta\cdot\nabla u_\ell-\lambda_\ell u_\ell)\overline{e_\ell^*}dx+\sum_{E\in\mathcal{E}_\ell}\int_E([\![\nabla u_\ell]\!]\cdot\nu_E)\overline{e_\ell^*}ds\\
&+\sum_{T\in\mathcal{T}_\ell}\int_T(-\beta\cdot\nabla\overline{u_\ell^*}-\overline{\lambda_\ell^*u_\ell^*})e_\ell dx+\sum_{E\in\mathcal{E}_\ell}\int_E([\![\nabla\overline{u_\ell^*}]\!]\cdot\nu_E)e_\ell ds\Bigg|.
\end{aligned}
$$

Proof. An integration by parts leads to

$$
\mathrm{Res}_\ell(e_\ell^*)=a(u_\ell,u^*-u_\ell^*)-\lambda_\ell b(u_\ell,u^*-u_\ell^*)=\sum_{T\in\mathcal{T}_\ell}\int_T(\beta\cdot\nabla u_\ell-\lambda_\ell u_\ell)\overline{(u^*-u_\ell^*)}dx+\sum_{E\in\mathcal{E}_\ell}\int_E[\nabla u_\ell]\cdot\nu_E\overline{(u^*-u_\ell^*)}ds.
$$

Similarly,

$$
\mathrm{Res}_\ell^*(e_\ell)=a(u-u_\ell,u_\ell^*)-\overline{\lambda_\ell^*}b(u-u_\ell,u_\ell^*)=\sum_{T\in\mathcal{T}_\ell}\int_T(-\beta\cdot\nabla\overline{u_\ell^*}-\overline{\lambda_\ell^*u_\ell^*})(u-u_\ell)dx+\sum_{E\in\mathcal{E}_\ell}\int_E[\nabla\overline{u_\ell^*}]\cdot\nu_E(u-u_\ell)ds. \qquad \square
$$

3.5. DWM estimator

Utilising the non standard Raviart–Thomas solution of an auxiliary problem leads to a new approach for a dual-weighted a posteriori error estimator. Note that this error estimator involves the unknown exact primal and dual errors e_ℓ and $\overline{e_\ell^*}$ as well as their unknown gradients ∇e_ℓ and $\nabla\overline{e_\ell^*}$. In practice these errors need to be approximated as described in Section 4.

Lemma 3.5. *Let the two mixed finite element functions $(q_M,u_M)\in RT_0(\mathcal{T}_\ell)\times\mathcal{P}_0(\mathcal{T}_\ell)$ and $(q_M^*,u_M^*)\in RT_0(\mathcal{T}_\ell)\times\mathcal{P}_0(\mathcal{T}_\ell)$ be the solutions of the equilibrium conditions*

$$
\begin{aligned}
&-div(q_M)+\beta\cdot q_M=f_\ell \text{ in }\Omega \quad\text{and}\quad q_M-\nabla u_M=0 \text{ in }\Omega,\\
&-div(q_M^*)-\beta\cdot q_M^*=f_\ell^* \text{ in }\Omega \quad\text{and}\quad q_M^*-\nabla u_M^*=0 \text{ in }\Omega,
\end{aligned}
$$

with right-hand sides $f_\ell,f_\ell^*\in\mathcal{P}_0(\mathcal{T}_\ell)$ given by $f_{\ell|T}:=h_T^{-2}\int_T\lambda_\ell u_\ell$ and $f_{\ell|T}^*:=h_T^{-2}\int_T\lambda_\ell^*u_\ell^*$ for $T\in\mathcal{T}_\ell$. Then the unknown exact errors e_ℓ and $\overline{e_\ell^*}$ satisfy

$$
\begin{aligned}
|\,\mathrm{Res}_\ell(e_\ell^*)+\mathrm{Res}_\ell^*(e_\ell)\,| \leqslant \Bigg| & \int_\Omega(\nabla u_\ell-q_M)\cdot\nabla\overline{e_\ell^*}dx+\int_\Omega(\overline{\nabla u_\ell^*-q_M^*})\cdot\nabla e_\ell dx+\int_\Omega\beta\cdot(\nabla u_\ell-q_M)\overline{e_\ell^*}dx\\
&-\int_\Omega\beta\cdot(\overline{\nabla u_\ell^*-q_M^*})e_\ell dx\Bigg|+\mathrm{HOT}
\end{aligned}
$$

with the higher-order term

$$
\mathrm{HOT}=\left|\int_\Omega(f_\ell-\lambda_\ell u_\ell)\overline{e_\ell^*}dx+\int_\Omega(\overline{f_\ell^*-\lambda_\ell^*u_\ell^*})e_\ell dx\right|.
$$

Proof. By the definition of the auxiliary problem for q_M and integration by parts it holds that

$$
\mathrm{Res}_\ell(e_\ell^*)=\int_\Omega\nabla u_\ell\cdot\nabla\overline{e_\ell^*}dx+\int_\Omega(\beta\cdot\nabla u_\ell-\lambda_\ell u_\ell)\overline{e_\ell^*}dx=\int_\Omega(\nabla u_\ell-q_M)\cdot\nabla\overline{e_\ell^*}dx+\int_\Omega\beta\cdot(\nabla u_\ell-q_M)\overline{e_\ell^*}dx+\int_\Omega(f_\ell-\lambda_\ell u_\ell)\overline{e_\ell^*}dx.
$$

Element-wise Cauchy and Poincaré [25] inequalities yield

$$
\int_\Omega(f_\ell-\lambda_\ell u_\ell)\overline{e_\ell^*}dx\leqslant\|f_\ell-\lambda_\ell u_\ell\|\|\overline{e_\ell^*}\|\leqslant\frac{1}{\pi}\left(\sum_{T\in\mathcal{T}_\ell}h_T^2\|\lambda_\ell\nabla u_\ell\|_{L^2(T)}^2\right)^{1/2}\|\overline{e_\ell^*}\|.
$$

Note that $\|\overline{e_\ell^*}\|$ is of the same convergence order as $|\,\lambda-\lambda_\ell\,|$ and that the last term involves an additional term of order $\mathcal{O}(H_\ell)$. Therefore, this term is formally of higher-order compared to $|\,\lambda-\lambda_\ell\,|$. The same argumentation leads to

$$\begin{aligned}\mathrm{Res}_\ell^*(e_\ell) &= \int_\Omega \nabla\overline{u_\ell^*}\cdot\nabla e_\ell dx + \int_\Omega(-\beta\cdot\nabla\overline{u_\ell^*} - \overline{\lambda_\ell^* u_\ell^*})e_\ell dx \\ &= \int_\Omega(\overline{\nabla u_\ell^* - q_M^*})\cdot\nabla e_\ell dx - \int_\Omega \beta\cdot(\overline{\nabla u_\ell^* - q_M^*})e_\ell dx + \int_\Omega(\overline{f_\ell^* - \lambda_\ell^* u_\ell^*})e_\ell dx.\end{aligned}$$

The last term is again a formally higher-order term. □

3.6. DWA estimator

The second new a posteriori error estimator makes use of the ideas of the DWR2 estimator. The new aspect proposed here is not to use integration by parts to obtain a residual term but to involve the averaged gradients $A(\nabla u_\ell)$ and $A(\nabla\overline{u_\ell^*})$ and then to do integration by parts. Again this error estimator involves the unknown exact primal and dual errors e_ℓ and $\overline{e_\ell^*}$ which have to be approximated as described in Section 4.

Lemma 3.6. *The unknown exact errors e_ℓ and $\overline{e_\ell^*}$ satisfy*

$$\begin{aligned}|\,\mathrm{Res}_\ell(e_\ell^*) + \mathrm{Res}_\ell^*(e_\ell)\,| = \Big| &\int_\Omega(\nabla u_\ell - A(\nabla u_\ell))\cdot\nabla\overline{e_\ell^*}dx + \int_\Omega(\nabla\overline{u_\ell^*} - A(\nabla\overline{u_\ell^*}))\cdot\nabla e_\ell dx \\ &+ \int_\Omega(-div(A(\nabla u_\ell)) + \beta\cdot\nabla u_\ell - \lambda_\ell u_\ell)\overline{e_\ell^*}dx + \int_\Omega(-div(A(\nabla\overline{u_\ell^*})) - \beta\cdot\nabla\overline{u_\ell^*} - \overline{\lambda_\ell^* u_\ell^*})e_\ell dx\Big|.\end{aligned}$$

Proof. An addition and subtraction of the averaging term $A(\nabla u_\ell)$ and an integration by parts yields

$$\mathrm{Res}_\ell(e_\ell^*) = a(u_\ell, u^* - u_\ell^*) - \lambda_\ell b(u_\ell, u^* - u_\ell^*) = \int_\Omega(\nabla u_\ell - A(\nabla u_\ell))\cdot\nabla\overline{e_\ell^*}dx + \int_\Omega(-div(A(\nabla u_\ell)) + \beta\cdot\nabla u_\ell - \lambda_\ell u_\ell)\overline{e_\ell^*}dx.$$

Analogously it follows

$$\mathrm{Res}_\ell^*(e_\ell) = a(u - u_\ell, u_\ell^*) - \overline{\lambda_\ell^*}b(u - u_\ell, u_\ell^*) = \int_\Omega(\nabla\overline{u_\ell^*} - A(\nabla\overline{u_\ell^*}))\cdot\nabla e_\ell dx + \int_\Omega(-div(A(\nabla\overline{u_\ell^*})) - \beta\cdot\nabla\overline{u_\ell^*} - \overline{\lambda_\ell^* u_\ell^*})e_\ell dx. \qquad \square$$

4. Adaptive finite element method

The adaptive finite element method (AFEM) generates a sequence of meshes $\mathcal{T}_0, \mathcal{T}_1, \ldots$ and associated discrete subspaces $V_0 \subsetneq V_1 \subsetneq \ldots \subsetneq V$ with discrete primal and discrete dual eigenpairs $(\lambda_\ell, u_\ell), (\lambda_\ell^*, u_\ell^*)$. A typical loop from V_ℓ to $V_{\ell+1}$ consists of the steps

SOLVE → ESTIMATE → MARK → REFINE.

4.1. Solve

The primal and dual generalized algebraic eigenvalue problems

$$A_\ell x_\ell = \lambda_\ell B_\ell x_\ell \quad\text{and}\quad y_\ell^H A_\ell = \overline{\lambda_\ell^*}y_\ell^H B_\ell$$

are solved with an algebraic eigensolver. Here, the coefficient matrices are the non-symmetric convection–diffusion matrix A_ℓ and the symmetric positive definite mass matrix B_ℓ. The right and left eigenvectors x_ℓ and y_ℓ represent the eigenfunctions

$$u_\ell = \sum_{k=1}^{\dim(V_\ell)} x_{\ell,k}\varphi_k \quad\text{and}\quad u_\ell^* = \sum_{k=1}^{\dim(V_\ell)} y_{\ell,k}\varphi_k,$$

with respect to the basis $(\varphi_1, \ldots, \varphi_{\dim(V_\ell)})$ of V_ℓ.

4.2. Estimate

Since the weight-terms e_ℓ and $\overline{e_\ell^*}$ in the dual-weighted a posteriori error estimators involve the unknown solutions u and $\overline{u^*}$, they have to be approximated. In the following experiments those functions are approximated by averaging $A(u_\ell) \in P_2(\mathcal{T}_\ell)$ of $u_\ell \in P_1(\mathcal{T}_\ell)$ and $A(\overline{u_\ell^*}) \in P_2(\mathcal{T}_\ell)$ of $\overline{u_\ell^*} \in P_1(\mathcal{T}_\ell)$ on the mesh $\mathcal{T}_\ell$. In contrast to the recovery of a gradient as in [33], the L^2 recovery of [32] is used here which is similar but uses different interpolation points. The post-processing is based on element patches $\omega_T := \cup_{z\subset T}\omega_z$ for $T \in \mathcal{T}_\ell$, where $\omega_z := \cup_{T\in\mathcal{T}_\ell; z\subset T} T$ is the nodal patch. The nodal and edge degrees of freedom for the interpolated $P_2(\mathcal{T}_\ell)$ function are computed for each element separately by a global least square quadratic

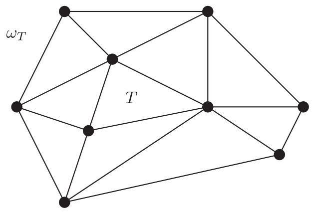

Fig. 1. Interpolation points for the element patch ω_T to the triangle $T \in \mathcal{T}_\ell$.

polynomial fitting. The interpolation points for the least square fitting are the nodal points of ω_T as displayed in Fig. 1. After all local values are computed, a global $P_2(\mathcal{T}_\ell)$ function is obtained by taking the arithmetic mean values for each node and midpoint of an edge of $\mathcal{T}_\ell$.

In [4] an alternative way of computing the estimator η_{DWR2} based on nodal values is presented. The analysis of this error estimator makes use of a special interpolation operator. This operator assumes that the mesh $\mathcal{T}_\ell$ results from uniform refinement of a coarser mesh and considers the nodal values as values for a higher-order P_2 basis on the coarser grid. The interpolation scheme presented here does not assumes any structure of the mesh.

The step ESTIMATE of the AFEM loop involves an appropriate a posteriori error estimator. In the numerical examples of Section 5 the following error estimators are compared. Since the residual identity depends on the eigenvalue condition number the condition number needs to be approximated for efficient a posteriori error control with efficiency indices close to one. In Section 5 it is shown empirically that the approximation $1/(2b(u_\ell, u_\ell^*))$ is efficient.

The first a posteriori error estimator is the residual estimator

$$\eta_{\ell,\mathrm{R}} = \frac{1}{2\mid b(u_\ell,u_\ell^*)\mid}\sum_{T\in\mathcal{T}}\left(h_T^2\|\beta\cdot\nabla u_\ell - \lambda_\ell u_\ell\|_{L^2(T)}^2 + \sum_{E\subset T} h_E\|[\![\nabla u_\ell]\!]\cdot\nu_E\|_{L^2(E)}^2\right)$$
$$+\frac{1}{2\mid b(u_\ell,u_\ell^*)\mid}\sum_{T\in\mathcal{T}}\left(h_T^2\|-\beta\cdot\nabla\overline{u_\ell^*} - \overline{\lambda_\ell^* u_\ell^*}\|_{L^2(T)}^2 + \sum_{E\subset T} h_E\|[\![\nabla\overline{u_\ell^*}]\!]\cdot\nu_E\|_{L^2(E)}^2\right).$$

The second a posteriori error estimator is the averaging estimator

$$\eta_{\ell,\mathrm{A}} = \frac{1}{2\mid b(u_\ell,u_\ell^*)\mid}\sum_{T\in\mathcal{T}}\left(\|A(\nabla u_\ell) - \nabla u_\ell\|_{L^2(T)}^2 + h_T^2\|-div(A(\nabla u_\ell)) + \beta\cdot\nabla u_\ell - \lambda_\ell u_\ell\|_{L^2(T)}^2\right)$$
$$+\frac{1}{2\mid b(u_\ell,u_\ell^*)\mid}\sum_{T\in\mathcal{T}}\left(\|A(\nabla\overline{u_\ell^*}) - \nabla\overline{u_\ell^*}\|_{L^2(T)}^2 + h_T^2\|-div(A(\nabla\overline{u_\ell^*})) - \beta\cdot\nabla\overline{u_\ell^*} - \overline{\lambda_\ell^* u_\ell^*}\|_{L^2(T)}^2\right).$$

The third a posteriori error estimator is the DWR1 estimator where the higher-order terms are neglected

$$\eta_{\ell,\mathrm{DWR1}} = \frac{1}{2\mid b(u_\ell,u_\ell^*)\mid}\left(\sum_{T\in\mathcal{T}_\ell} h_T^{3/2}\eta_T\|[\nabla u_\ell^*]\cdot\nu_E\|_{L^2(\partial T)} + \sum_{T\in\mathcal{T}_\ell} h_T^{3/2}\eta_T^*\|[\nabla u_\ell]\cdot\nu_E\|_{L^2(\partial T)}\right),$$

with η_T and η_T^* from (3.2).

The fourth a posteriori error estimator is the DWR2 estimator where the unknown solutions in the weights, u and u^*, are interpolated by $A(\overline{u_\ell^*})$ and $A(\overline{u_\ell^*})$ as described above

$$\eta_{\ell,\mathrm{DWR2}} = \frac{1}{2\mid b(u_\ell,u_\ell^*)\mid}\left|\sum_{E\in\mathcal{E}_\ell}\int_E([\![\nabla u_\ell]\!]\cdot\nu_E)(A(\overline{u_\ell^*}) - \overline{u_\ell^*})ds + \sum_{E\in\mathcal{E}_\ell}\int_E([\![\nabla\overline{u_\ell^*}]\!]\cdot\nu_E)(A(u_\ell) - u_\ell)ds\right.$$
$$\left.+\sum_{T\in\mathcal{T}_\ell}\int_T(\beta\cdot\nabla u_\ell - \lambda_\ell u_\ell)(A(\overline{u_\ell^*}) - \overline{u_\ell^*})dx + \sum_{T\in\mathcal{T}_\ell}\int_T(-\beta\cdot\nabla\overline{u_\ell^*} - \overline{\lambda_\ell^* u_\ell^*})(A(u_\ell) - u_\ell)dx\right|.$$

The local refinement indicators read

$$\eta_T := \left|\int_T(\beta\cdot\nabla u_\ell - \lambda_\ell u_\ell)(A(\overline{u_\ell^*}) - \overline{u_\ell^*})dx + \sum_{E\in\partial T}\int_E([\![\nabla u_\ell]\!]\cdot\nu_E)(A(\overline{u_\ell^*}) - \overline{u_\ell^*})ds + \int_T(-\beta\cdot\nabla\overline{u_\ell^*} - \overline{\lambda_\ell^* u_\ell^*})(A(u_\ell) - u_\ell)dx\right.$$
$$\left.+\sum_{E\in\partial T}\int_E([\![\nabla\overline{u_\ell^*}]\!]\cdot\nu_E)(A(u_\ell) - u_\ell)ds\right|.$$

They are only necessary to determine the set of marked edges for refinement.

The fifth a posteriori error estimator utilised the auxiliary Raviart–Thomas mixed solutions q_M and q_M^* and the averaged gradients $A(\nabla u_\ell)$ and $A(\nabla\overline{u_\ell^*})$

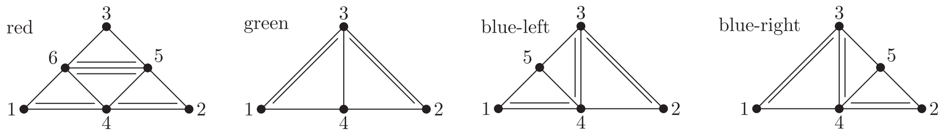

Fig. 2. Refinement rules: sub-triangles with corresponding reference edges depicted with a second edge.

$$\eta_{\ell,\mathrm{DWM}} = \frac{1}{2\mid b(u_\ell,u_\ell^*)\mid}\left|\int_\Omega(\nabla u_\ell - q_M)\cdot(A(\nabla\overline{u_\ell^*}) - \nabla\overline{u_\ell^*})dx + \int_\Omega(\overline{\nabla u_\ell^* - q_M^*})\cdot(A(\nabla u_\ell) - \nabla u_\ell)dx \right.$$
$$\left. + \int_\Omega \beta\cdot(\nabla u_\ell - q_M)(A(\overline{u_\ell^*}) - \overline{u_\ell^*})dx - \int_\Omega \beta\cdot(\overline{\nabla u_\ell^* - q_M^*})(A(u_\ell) - u_\ell)dx\right|,$$

where the higher-order term is neglected. The local refinement indicators read

$$\eta_T := \left|\int_T(\nabla u_\ell - q_M)\cdot\nabla(A(\nabla\overline{u_\ell^*}) - \nabla\overline{u_\ell^*})dx + \int_T(\overline{\nabla u_\ell^* - q_M^*})\cdot(A(\nabla u_\ell) - \nabla u_\ell)dx \right.$$
$$\left. + \int_T \beta\cdot(\nabla u_\ell - q_M)(A(\overline{u_\ell^*}) - \overline{u_\ell^*})dx - \int_T \beta\cdot(\overline{\nabla u_\ell^* - q_M^*})(A(u_\ell) - u_\ell)dx\right|.$$

The last error a posteriori error estimator uses both averaged gradients $A(\nabla u_\ell)$ and $A(\nabla\overline{u_\ell^*})$ as well as interpolated L^2 functions $A(u_\ell^*)$ and $A(\overline{u_\ell^*})$ for the weights

$$\mu_{\ell,\mathrm{DWA}} = \frac{1}{2\mid b(u_\ell,u_\ell^*)\mid}\left|\int_\Omega(\nabla u_\ell - A(\nabla u_\ell))\cdot(A(\nabla\overline{u_\ell^*}) - \nabla\overline{u_\ell^*})dx + \int_\Omega(\nabla\overline{u_\ell^*} - A(\nabla\overline{u_\ell^*}))\cdot(A(\nabla u_\ell) - \nabla u_\ell)dx \right.$$
$$\left. + \int_\Omega(-div(A(\nabla u_\ell)) + \beta\cdot\nabla u_\ell - \lambda_\ell u_\ell)(A(\overline{u_\ell^*}) - \overline{u_\ell^*})dx + \int_\Omega(-div(A(\nabla\overline{u_\ell^*})) - \beta\cdot\nabla\overline{u_\ell^*} - \overline{\lambda_\ell^* u_\ell^*})(A(u_\ell) - u_\ell)dx\right|.$$

Here, the local refinement indicators read

$$\eta_T := \left|\int_T(\nabla u_\ell - A(\nabla u_\ell))\cdot(A(\nabla\overline{u_\ell^*}) - \nabla\overline{u_\ell^*})dx + \int_T(\nabla\overline{u_\ell^*} - A(\nabla\overline{u_\ell^*}))\cdot(A(\nabla u_\ell) - \nabla u_\ell)dx \right.$$
$$\left. + \int_T(-div(A(\nabla u_\ell))\beta\cdot\nabla u_\ell - \lambda_\ell u_\ell)(A(\overline{u_\ell^*}) - \overline{u_\ell^*})dx + \int_T(-div(A(\nabla\overline{u_\ell^*})) - \beta\cdot\nabla\overline{u_\ell^*} - \overline{\lambda_\ell^* u_\ell^*})(A(u_\ell) - u_\ell)dx\right|.$$

4.3. Mark

Based on the refinement indicators, the set of elements $\mathcal{M}_\ell \subseteq \mathcal{T}_\ell$ that are refined is specified in the algorithm `Mark`. Let $\mathcal{M}_\ell$ be the set of minimal cardinality for which the bulk criterion [12],

$$\theta\sum_{T\in\mathcal{T}_\ell}\eta_T^2 \leqslant \sum_{T\in\mathcal{M}_\ell}\eta_T^2$$

is satisfied for a given bulk parameter $0 < \theta \leqslant 1$.

4.4. Refine

Given the set $\mathcal{M}_\ell \subseteq \mathcal{T}_\ell$ of marked elements, mark all edges of elements in $\mathcal{M}_\ell$ for refinement. The closure algorithm computes a superset of refined edges such that once an edge of a triangle is marked for refinement its reference edge is marked as well. The refinement $\mathcal{T}_{\ell+1}$ is obtained by application of the refinement rules from Fig. 2.

5. Numerical experiments

This section is devoted to numerical experiments and the empirical evidence of reliability, efficiency and stability for higher eigenvalues and strong convection coefficients. The numerical experiments on the unit square investigate the validity of the residual identity of Lemma 2.1 and the efficiency of the proposed eigenvalue condition number approximation. The experiments of the L shaped domain investigate the stability of the a posteriori error estimators for higher eigenvalues and the experiments on the slit domain their robustness in β.

5.1. Unit square

As first example consider the convection–diffusion eigenvalue model problem (1.1) on the unit square $\Omega = (0,1)\times(0,1)$. For constant convection coefficient β, the exact eigenvalue with smallest real part reads $\lambda = \mid\beta\mid^2/4 + 2\pi^2$ [26]. The corresponding primal and dual eigenfunctions read

$$u(x,y) = \exp\left(\frac{\beta \cdot (x,y)^t}{2}\right) \sin(\pi x) \sin(\pi y),$$

$$u^*(x,y) = \exp\left(-\frac{\beta \cdot (x,y)^t}{2}\right) \sin(\pi x) \sin(\pi y).$$

Two discrete primal and dual solutions are displayed in Fig. 3. To investigate the stability of the residual equation of Lemma 2.1 which depends on the condition number of the eigenvalue Fig. 4 shows the factor

$$\left(b(u,u^*) + b(u_\ell, u_\ell^*) - b(e_\ell, e_\ell^*)\right)^{-1}$$

for different values of β. The values depend strongly on the size of $|\beta|$ and eigenvalue computations beyond $|\beta| \gg 20$ is numerically unstable. Fig. 5 compares the accuracy of the eigenvalue condition number approximation $(2b(u_\ell, u_\ell^*))^{-1}$ with the error

$$\delta_\ell := \left(b(u,u^*) + b(u_\ell, u_\ell^*) - b(e_\ell, e_\ell^*)\right)^{-1} - (2b(u_\ell, u_\ell^*))^{-1}$$

compared to the eigenvalue error. Since the error for the eigenvalue condition number is much smaller than the eigenvalue error for different values of β, the proposed approximation $(2b(u_\ell, u_\ell^*))^{-1}$ of the eigenvalue condition number is empirical efficient. In all presented numerical results the sign of $\mathrm{Res}_\ell(e_\ell^*)$ and $\mathrm{Res}_\ell^*(e_\ell)$ is in fact the same. Thus the triangle inequality $|\mathrm{Res}_\ell(e_\ell^*) + \mathrm{Res}_\ell^*(e_\ell)| \leqslant |\mathrm{Res}_\ell(e_\ell^*)| + |\mathrm{Res}_\ell^*(e_\ell)|$ in the proof of Theorem 2.4 does not destroy the efficiency of the estimate. Let N_ℓ denote the number of unknowns, i.e., the number of inner nodes. Because the domain is convex, even uniform refinement results in optimal convergence rates of $\mathcal{O}(N_\ell^{-1})$ as shown in Fig. 6. Note that for uniform meshes $N_\ell \approx h_\ell^{-2}$ and that there is some strong pre-asymptotic error due to the eigenvalue condition number estimate. The a posteriori error estimators $\eta_{\ell,\mathrm{DWR2}}, \eta_{\ell,\mathrm{DWM}}$, and $\eta_{\ell,\mathrm{DWA}}$ are close to the error while $\eta_{\ell,\mathrm{R}}, \eta_{\ell,\mathrm{A}}$, and $\eta_{\ell,\mathrm{DWR1}}$ are by factors $10^4 - 10^6$ larger than the error. Note that the first term of the error estimator $\eta_{\ell,\mathrm{A}}$ is of higher order and $\eta_{\ell,\mathrm{A}}$ is asymptotically reliable.

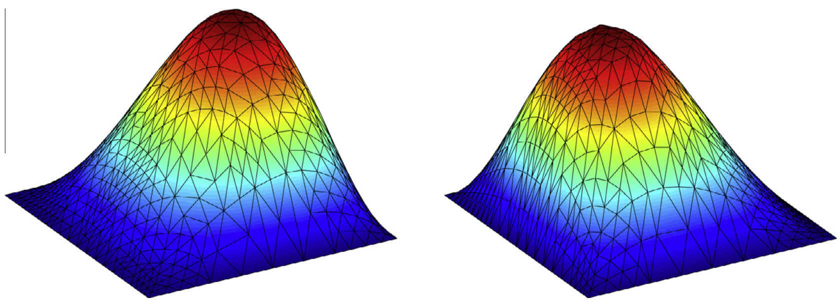

Fig. 3. Primal (left) and dual (right) discrete solution for $\beta = (3,0)$ on adaptively refined meshes generated by $\eta_{\ell,\mathrm{R}}$ on the unit square with about 500 nodes.

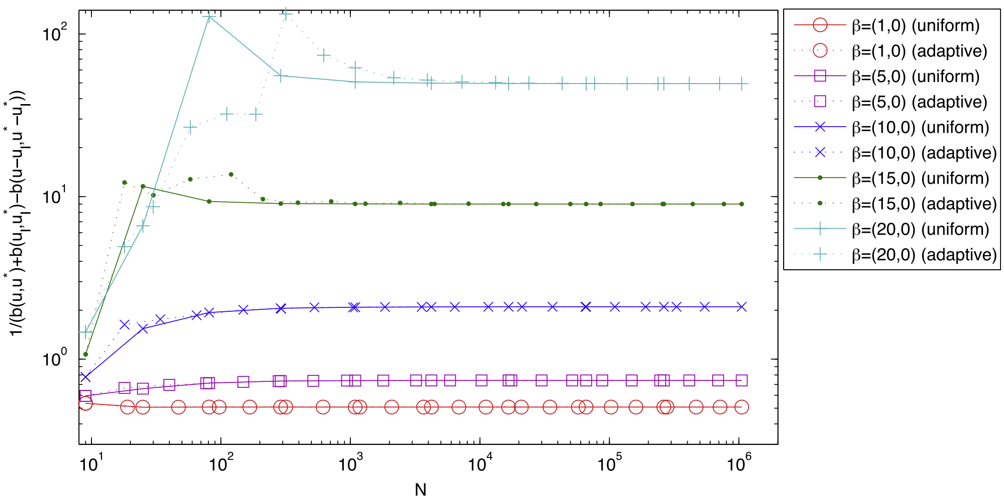

Fig. 4. Eigenvalue condition numbers for different values of β and sequences of uniform and adaptive meshes generated by $\eta_{\ell,\mathrm{R}}$ on the unit square.

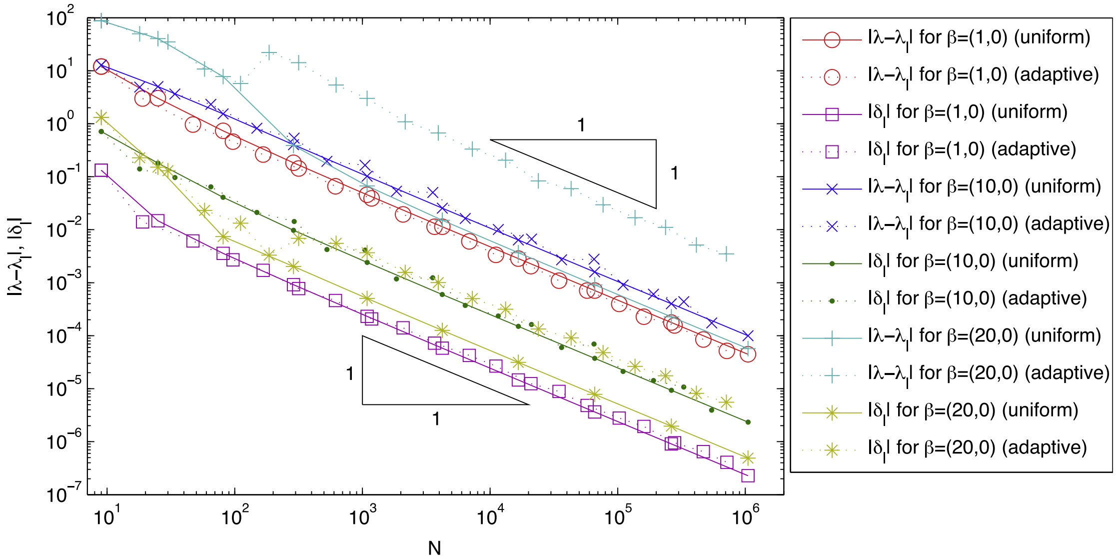

Fig. 5. Eigenvalue errors and $|\delta_\ell|$ for different values of β and sequences of uniform and adaptive meshes generated by $\eta_{\ell,\mathrm{R}}$ on the unit square.

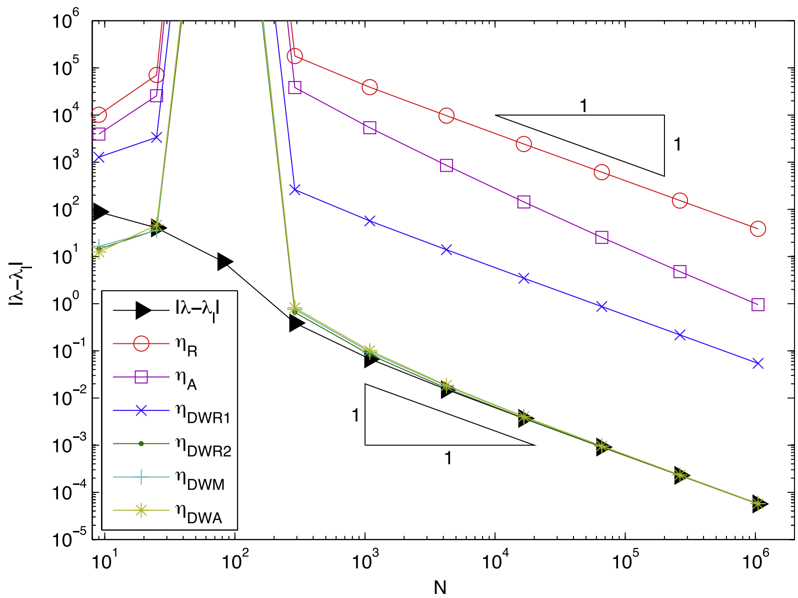

Fig. 6. Eigenvalue errors and error estimators for $\beta = (20,0)$ and a sequence of uniform meshes on the unit square.

5.2. L-shaped domain

The second example is the convection–diffusion eigenvalue model problem (1.1) on the L-shaped domain $\Omega = ((-1,1)\times(-1,1)) \setminus ([0,1]\times[0,-1])$ with constant convection parameter $\beta = (3,0)$ and higher eigenvalues. The primal and dual solutions for adaptive meshes generated by the AFEM, based on the a posteriori error estimator $\eta_{\ell,\mathrm{DWR2}}$ for the 5-th eigenvalue with smallest real part, are shown in Fig. 7. An approximation of the first eigenvalue reads $\lambda = |\beta|^2/4 + 9.6397238$ where 9.6397238 from [30] is an approximation of the first Laplace eigenvalue. In Fig. 8 it is shown that uniform refinement results in a suboptimal convergence rate of about $\mathcal{O}(N_\ell^{-2/3})$, while adaptive refinement leads to numerically optimal convergence rates of $\mathcal{O}(N_\ell^{-1})$. The experiments show that the a posteriori error estimators are reliable and efficient for adaptive mesh refinement. Notice that the eigenvalues obtained from the AFEM for different estimators lead to similar eigenvalue errors. As before the values of $\eta_{\ell,\mathrm{DWR2}}, \eta_{\ell,\mathrm{DWM}}$, and $\eta_{\ell,\mathrm{DWA}}$ are closer to the exact error than those of

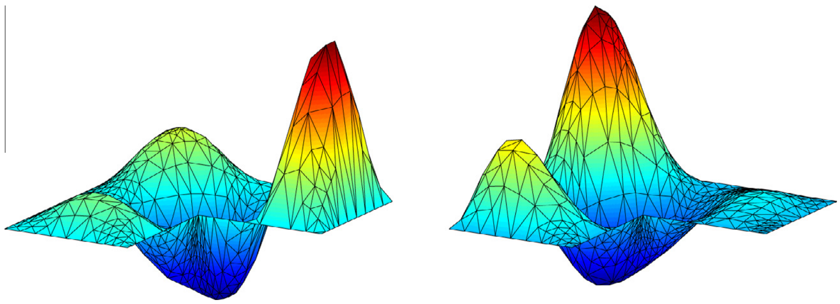

Fig. 7. Primal (left) and dual (right) discrete solution for $\beta = (3,0), \lambda_5$ on adaptively refined meshes generated by $\eta_{\ell,\mathrm{DWR2}}$ on the L-shaped domain with about 500 nodes.

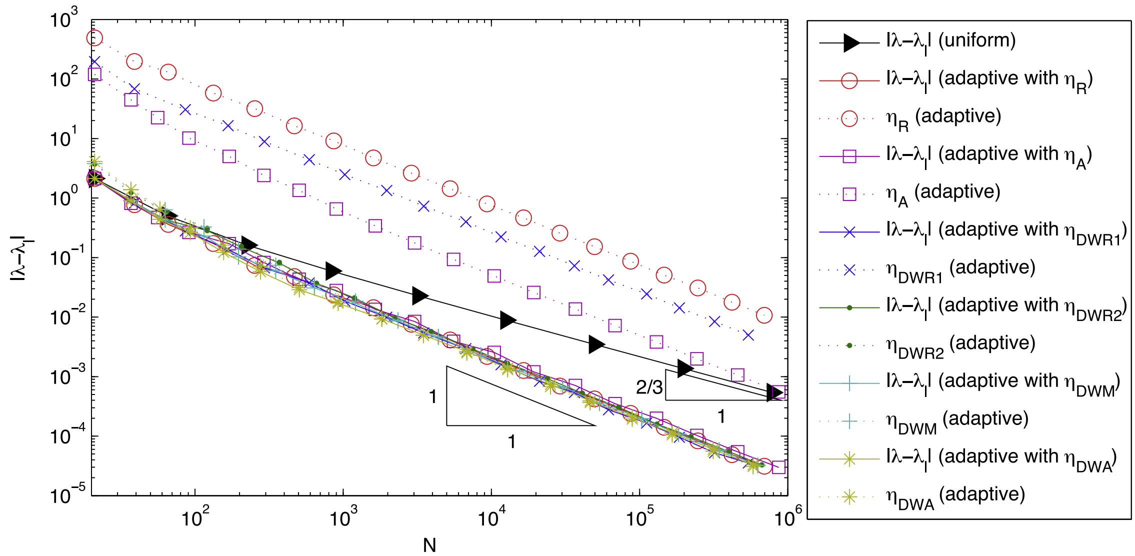

Fig. 8. Eigenvalue errors and estimators for $\beta = (3,0), \lambda_1$ and sequences of uniform and adaptive meshes on the L-shaped domain.

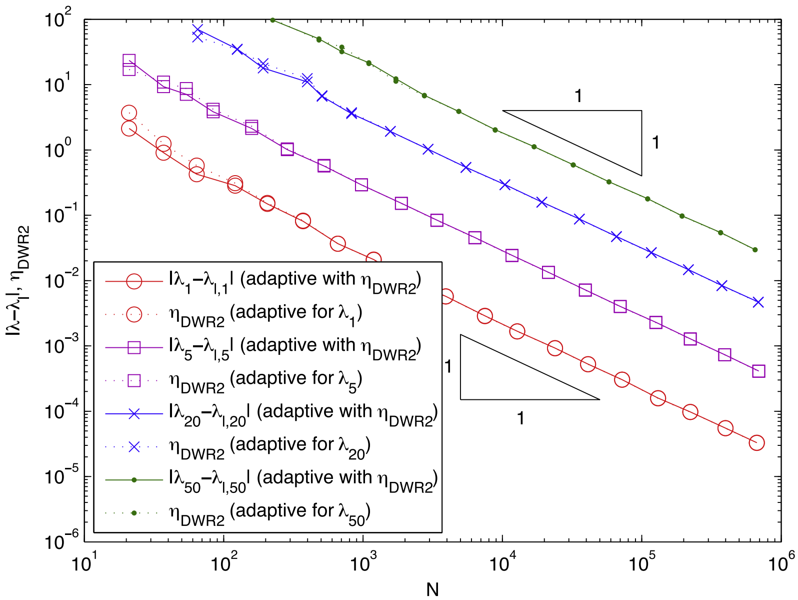

Fig. 9. Eigenvalue errors for $\beta = (3,0), \lambda_1, \lambda_5, \lambda_{20}$ and λ_{50} for sequences of uniform and adaptive meshes generated by $\eta_{\ell,\mathrm{DWR2}}$ on the L-shaped domain.

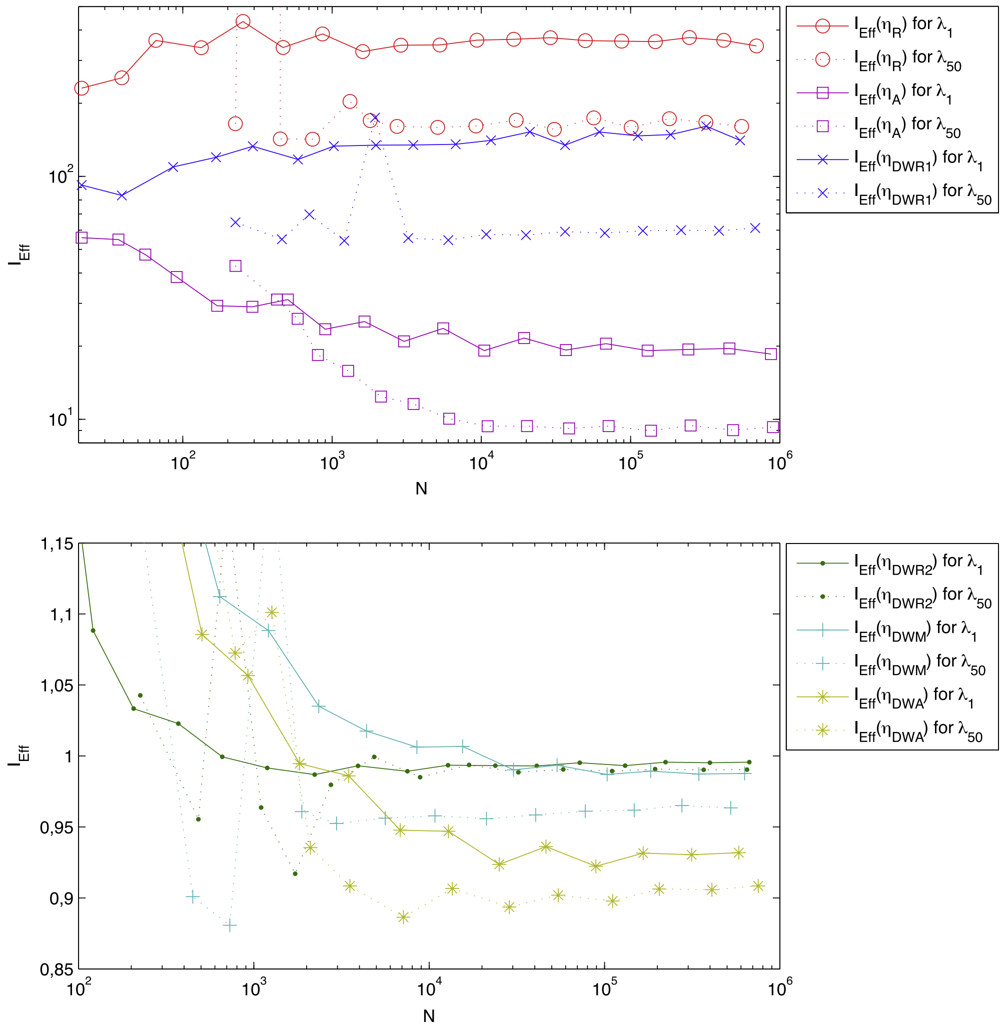

Fig. 10. Efficiency indices I_{Eff} for $\beta = (3,0), \lambda_1, \lambda_{50}$ and adaptive meshes on the L-shaped domain.

$\eta_{\ell,R}, \eta_{\ell,A}$, and $\eta_{\ell,DWR1}$. In order to study the dependence of the a posteriori error estimators on the size of the eigenvalue, we compare the numerical results for

$$\lambda_1 = |\beta|^2/4 + 9.6397238, \quad \lambda_5 = |\beta|^2/4 + 31.912636,$$
$$\lambda_{20} = |\beta|^2/4 + 101.60529, \quad \lambda_{50} = |\beta|^2/4 + 250.78548,$$

with approximations for the corresponding Laplace eigenvalues from [30]. Fig. 9 shows that the size of the eigenvalue error depends on the eigenvalue and that the a posteriori error estimator $\eta_{\ell,DWR2}$ is asymptotically exact. In order to investigate the dependence on the size of the eigenvalue, the efficiency indices $I_{Eff} = \eta_\ell / |\lambda - \lambda_\ell|$ for λ_1 and λ_{50} are compared in Fig. 10. The experiments show that the ratio between the a posteriori error estimators and the eigenvalue error is growing in λ for $\eta_{\ell,R}, \eta_{\ell,A}$, and $\eta_{\ell,DWR1}$ while $\eta_{\ell,DWR2}, \eta_{\ell,DWM}$, and $\eta_{\ell,DWA}$ are robust in λ. Note that the efficiency indices of $\eta_{\ell,DWR2}, \eta_{\ell,DWM}$, and $\eta_{\ell,DWA}$ are close to one.

5.3. Slit domain

As last example consider the convection–diffusion eigenvalue model problem (1.1) on the slit domain $\Omega = ((-1,1)\times(-1,1)) \setminus ([0,1]\times\{0\})$ with different constant values for β. A computed reference value for the first eigenvalue reads $\lambda = |\beta|^2/4 + 8.3713297112$ with approximation 8.3713297112 of the first Laplace eigenvalue computed on very fine meshes and higher order finite elements. The primal and dual eigenfunctions on adaptive meshes for $\eta_{\ell,DWA}$ are shown in Fig. 11. Notice that for the primal eigenfunction the influence of the magnitude of the corner singularity at the origin is much larger than for the dual eigenfunction. This illustrates that it is important to consider both primal and dual residuals. Due to

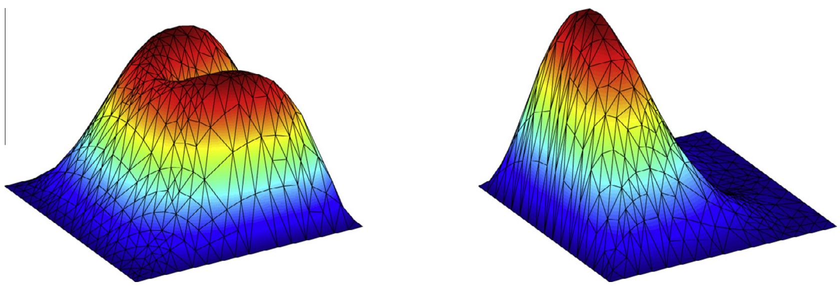

Fig. 11. Primal (left) and dual (right) discrete solution for $\beta = (3, 0)$ on adaptively refined meshes generated by $\eta_{\ell,\mathrm{DWA}}$ on the slit domain with about 500 nodes.

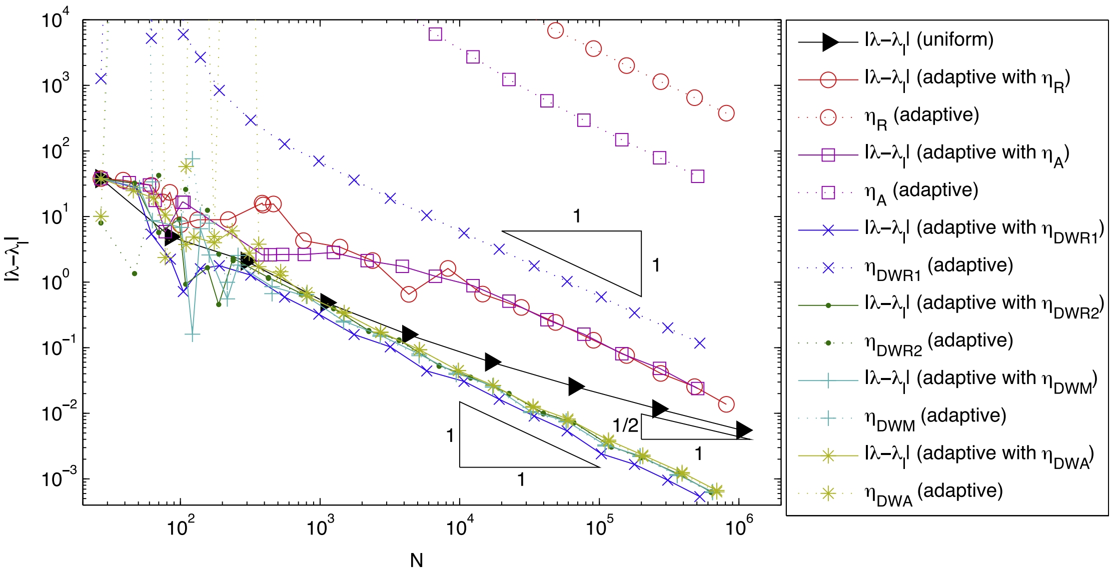

Fig. 12. Eigenvalue errors and estimators for $\beta = (15, 0)$ and sequences of uniform and adaptive meshes on the slit domain.

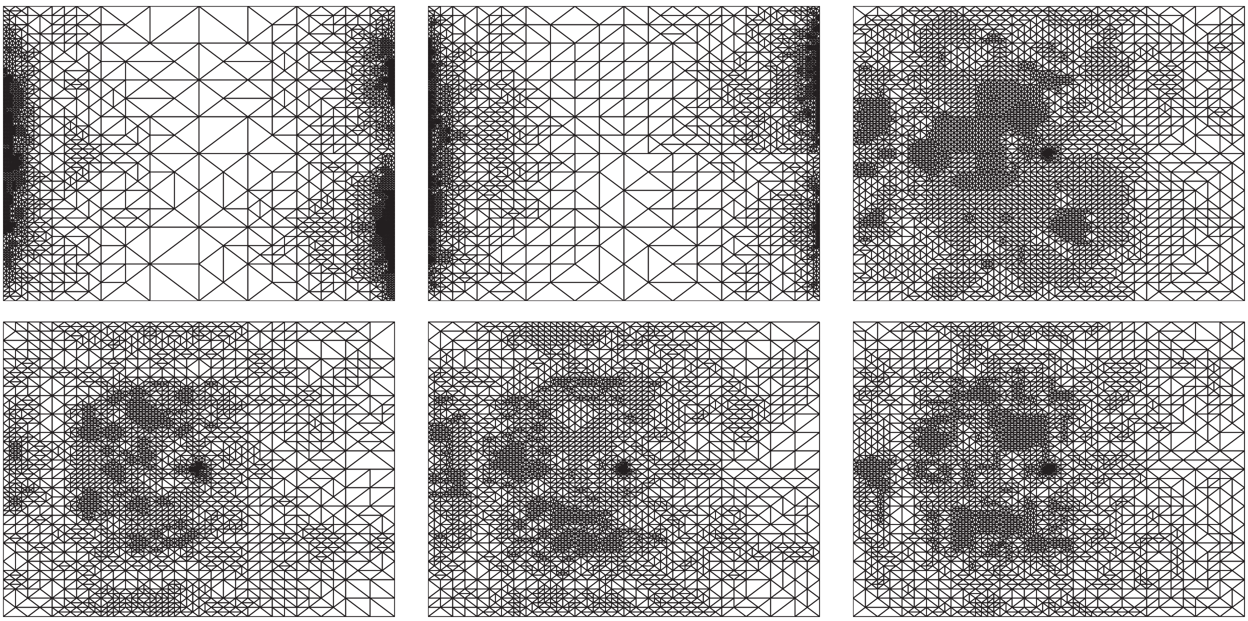

Fig. 13. Meshes with $\beta = (15, 0)$ generated by the refinement monitored by $\eta_{\ell,R}, \eta_{\ell,A}, \eta_{\ell,\mathrm{DWR1}}, \eta_{\ell,\mathrm{DWR2}}, \eta_{\ell,\mathrm{DWM}}$ and $\eta_{\ell,\mathrm{DWA}}$ (from left to right and top to bottom) on the Slit domain with about 2500 nodes.

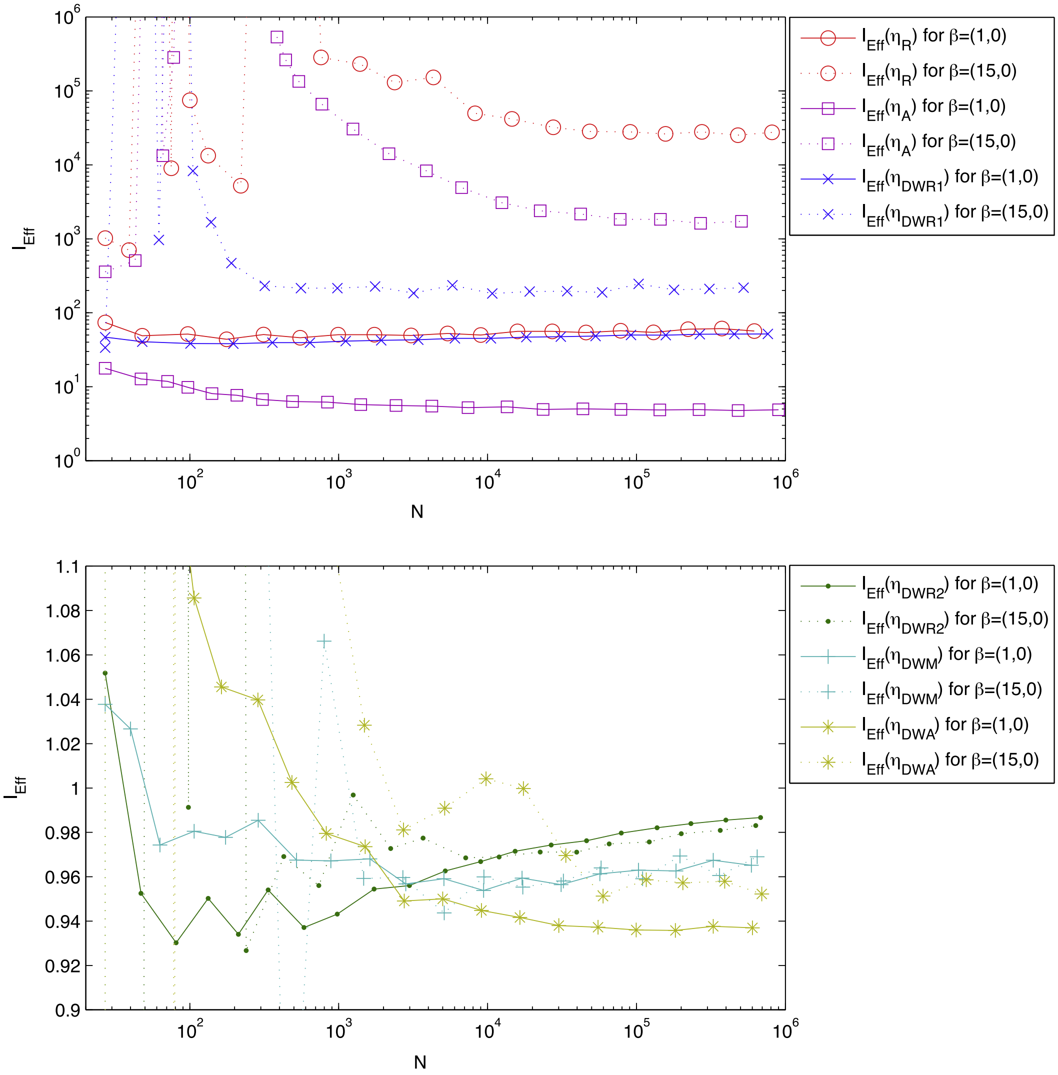

Fig. 14. Efficiency indices $\mathrm{I_{Eff}}$ for $\beta = (1,0), (15,0)$ and adaptive sequences of meshes on the slit domain.

the corner singularity, uniform refinement results in a suboptimal convergence rate $\mathcal{O}(N_\ell^{-1/2})$ while adaptive refinement results in the optimal convergence rate $\mathcal{O}(N_\ell^{-1})$ as shown in Fig. 12 for $\beta = (15,0)$. Note that the eigenvalue errors for $\eta_{\ell,\mathrm{R}}$ and $\eta_{\ell,\mathrm{A}}$ are much larger than for $\eta_{\ell,\mathrm{DWR1}}, \eta_{\ell,\mathrm{DWR2}}, \eta_{\ell,\mathrm{DWM}}$ and $\eta_{\ell,\mathrm{DWA}}$ and even larger than the eigenvalue error for uniform refinement up to $\mathcal{N}_\ell = 10^6$. This observation is caused by a much larger pre-asymptotic range for $\eta_{\ell,\mathrm{R}}$ and $\eta_{\ell,\mathrm{A}}$ than for the DWR based a posteriori error estimators. The different adaptive meshes with about $\mathcal{N}_\ell = 2500$ are shown in Fig. 13. The meshes for $\eta_{\ell,\mathrm{R}}$ and $\eta_{\ell,\mathrm{A}}$ show strong refinement towards the two boundary layers on the left and right but almost no refinement towards the corner singularity at the origin which might cause the larger eigenvalue errors. In contrast to that all other refinement indicators show strong refinement toward the corner singularity at the origin which leads to smaller eigenvalue errors. In order to study the dependence of the a posteriori error estimators on the size of the convection coefficient, experiments for $\beta = (1,0)$ and $\beta = (15,0)$ are compared in Fig. 14. The constants of the estimates in Lemma 3.1 and Lemma 3.2 depend on the size of the convection parameter. Thus, the efficiency indices I_{eff} are expected to depend on the size of $|\beta|$ as well which is confirmed by the numerical experiments. The size of the efficiency indices grows for the a posteriori error estimators $\eta_{\ell,\mathrm{R}}, \eta_{\ell,\mathrm{A}}$ and $\eta_{\ell,\mathrm{DWR1}}$ corresponding to the increase of $|\beta|$. In contrast the efficiency indices for $\eta_{\ell,\mathrm{DWR2}}, \eta_{\ell,\mathrm{DWM}}$ and $\eta_{\ell,\mathrm{DWA}}$ are robust in β and asymptotically close to one.

6. Conclusions

All the numerical results indicate that the a posteriori error estimators are empirically reliable and efficient for sufficiently small global mesh-size. The interpolation scheme of Section 4 for the weights shows to be empirical stable for unstructured triangular meshes. The approximation of the condition number needs to be included in the a posteriori error estimators in order to get efficiency indices close to one. The DWR2, DWM and the DWA a posteriori error estimators result in the best asymptotic efficiency indices close to one independently of both, the size of the eigenvalue and the convection parameter. For larger values of $|\beta|$ the DWR based a posteriori error estimators show much better results than the residual and averaging based a posteriori error estimators because of the much smaller pre-asymptotic range. Since the used eigenvalue solver ARPACK [21] shows some instability for convection coefficients larger than $(20,0)$ and coarser meshes those are excluded in this paper. For highly non-symmetric problems other techniques such as homotopy methods [10] need to be applied in order to compute the same eigenvalue of interest during all steps of the adaptive finite element loop or different finite elements need to be considered such as discontinuous Galerkin finite elements [11].

Acknowledgements

The authors thank V. Mehrmann and A. Miedlar from TU Berlin and R. Rannacher from University of Heidelberg for inspiring discussions. The authors also thank the anonymous referees for their valuable comments and suggestions.

References

[1] W. Bangerth, R. Rannacher, Adaptive Finite Element Methods for Differential Equations, Birkhäuser, Basel, 2003.
[2] R. Becker, R. Rannacher, Weighted a posteriori error control in FE methods, Hans Georg et al. (Ed.), ENUMATH 97, 1998.
[3] R. Becker, R. Rannacher, An optimal control approach to error estimation and mesh adaptation in finite element methods, Acta Numerica 2000, Cambridge University Press, 2001.
[4] M. Braack, A. Ern, A posteriori control of modeling errors and discretization errors, Multiscale Model. Simul. 1 (2) (2003) 221–238.
[5] S.C. Brenner, L.R. Scott, The Mathematical Theory of Finite Element Methods, second ed., Texts in Applied Mathematics, Springer-Verlag, 2002.
[6] F. Brezzi, M. Fortin, Mixed and Hybrid Finite Element Methods, Springer Series in Computational Mathematics, vol. 15, Springer-Verlag, New York, 1991.
[7] C. Carstensen, All first-order averaging techniques for a posteriori finite element error control on unstructured grids are efficient and reliable, Math. Comput. 73 (2003) 1153–1165.
[8] C. Carstensen, Estimation of higher Sobolev norm from lower order approximation, SIAM J. Numer. Anal. 42 (5) (2005) 2136–2147.
[9] C. Carstensen, J. Gedicke, An oscillation-free adaptive FEM for symmetric eigenvalue problems, Numer. Math. 118 (3) (2011) 401–427.
[10] C. Carstensen, J. Gedicke, V. Mehrmann, A. Miedlar, An adaptive homotopy approach for non-selfadjoint eigenvalue problems, Numer. Math. 119 (3) (2011) 557–583.
[11] K.A. Cliffe, E.J.C. Hall, P. Houston, Adaptive discontinuous Galerkin methods for eigenvalue problems arising in incompressible fluid flows, SIAM J. Sci. Comput. 31 (6) (2009/10) 4607–4632.
[12] W. Dörfler, A convergent adaptive algorithm for Poisson's equation, SIAM J. Numer. Anal. 33 (3) (1996) 1106–1124.
[13] R.G. Durán, C. Padra, R. Rodríguez, A posteriori error estimates for the finite element approximation of eigenvalue problems, Math. Models Methods Appl. Sci. 13 (8) (2003) 1219–1229.
[14] E.M. Garau, P. Morin, C. Zuppa, Convergence of adaptive finite element methods for eigenvalue problems, Math. Models Methods Appl. Sci. 19 (5) (2009) 721–747.
[15] S. Giani, I.G. Graham, A convergent adaptive method for elliptic eigenvalue problems, SIAM J. Numer. Anal. 47 (2009) 1067–1091.
[16] G.H. Golub, C.F. Van Loan, Matrix computations, Johns Hopkins Studies in the Mathematical Sciences, third ed., Johns Hopkins University Press, Baltimore, MD, 1996.
[17] V. Heuveline, R. Rannacher, A posteriori error control for finite element approximations of elliptic eigenvalue problems, Adv. Comput. Math. 15 (2001) 107–138.
[18] V. Heuveline, R. Rannacher, Adaptive FEM for eigenvalue problems, in: Numerical Mathematics and Advanced Applications, Springer, Italia, Milan, 2003, pp. 713–722.
[19] T. Kato, Pertubation Theory for linear Operators, Springer, 1980.
[20] M.G. Larson, A posteriori and a priori error analysis for finite element approximations of self-adjoint elliptic eigenvalue problems, SIAM J. Numer. Anal. 38 (2000) 608–625.
[21] R.B. Lehoucq, D.C. Sorensen, C. Yang, ARPACK Users' Guide: Solution of Large-Scale Eigenvalue Problems with Implicitly Restarted Arnoldi Methods, SIAM, 1998.
[22] D. Mao, L. Shen, A. Zhou, Adaptive finite element algorithms for eigenvalue problems based on local averaging type a posteriori error estimates, Adv. Comput. Math. 25 (2006) 135–160.
[23] J.T. Oden, S. Prudhomme, T. Westermann, J. Bass, M.E. Botkin, Error estimation of eigenfrequencies for elasticity and shell problems, Math. Models Methods Appl. Sci. 13 (3) (2003) 323–344.
[24] J.E. Osborn, I. Babuška, Eigenvalue Problems, Handbook of Numerical Analysis, vol 2, 1991.
[25] L.E. Payne, H.F. Weinberger, An optimal Poincaré inequality for convex domains, Arch. Ration. Mech. Anal. 5 (1960) 286–292.
[26] R. Rannacher, A. Westenberger, W. Wollner, Adaptive finite element solution of eigenvalue problems: balancing of discretization and iteration error, J. Numer. Math. 18 (4) (2010) 303–327.
[27] P.-A. Raviart, J.M. Thomas, A mixed finite element method for 2nd order elliptic problems, in: Mathematical Aspects of Finite Element Methods (Proc. Conf., Consiglio Naz. delle Ricerche (C.N.R.), Rome, 1975), Lecture Notes in Math., vol. 606, Springer, Berlin, 1977, pp. 292–315.
[28] S. Sauter, hp-finite elements for elliptic eigenvalue problems: error estimates which are explicit with respect to h and p, SIAM J. Numer. Anal. 48 (1) (2010) 95–108.
[29] L.R. Scott, S. Zhang, Finite element interpolation of nonsmooth functions satisfying boundary conditions, Math. Comput. 54 (190) (1990) 483–493.
[30] L.N. Trefethen, T. Betcke, Computed eigenmodes of planar regions, in: Recent Advances in Differential Equations and Mathematical Physics, Contemp. Math., vol. 412, Amer. Math. Soc., 2006, pp. 297–314.
[31] R. Verfürth, A Review of A Posteriori Error Estimation and Adaptive Mesh-Refinement Techniques, Wiley and Teubner, 1996.
[32] N.-E. Wiberg, X.D. Li, Superconvergent patch recovery of finite-element solution and a posteriori L_2 norm error estimate, Commun. Numer. Methods Engrg. 10 (4) (1994) 313–320.
[33] O.C. Zienkiewicz, J.Z. Zhu, The superconvergent patch recovery and a posteriori error estimates. Part 1: The recovery technique, Int. J. Numer. Methods Engrg. 33 (1992) 1331–1364.